



Justus-Liebig-Universität Gießen

Fachbereich Biologie und Chemie

Institut für Anorganische und Analytische Chemie

---

# Kinetic Investigations of Nickel and Iron Complexes with Olefinic and Macrocyclic Ligands

Kumulativ-Dissertation zur Erlangung  
des Doktorgrades der Naturwissenschaften

vorgelegt von

**Florian Josef Ritz**

aus Hünfeld

November 2023

## Selbstständigkeitserklärung

Ich erkläre: Ich habe die vorgelegte Dissertation selbstständig und ohne unerlaubte fremde Hilfe und nur mit den Hilfen angefertigt, die ich in der Dissertation angegeben habe. Alle Textstellen, die wörtlich oder sinngemäß aus veröffentlichten Schriften entnommen sind, und alle Angaben, die auf mündlichen Auskünften beruhen, sind als solche kenntlich gemacht. Ich stimme einer evtl. Überprüfung meiner Dissertation durch eine Antiplagiat-Software zu. Bei den von mir durchgeführten und in der Dissertation erwähnten Untersuchungen habe ich die Grundsätze guter wissenschaftlicher Praxis, wie sie in der „Satzung der Justus-Liebig-Universität Gießen zur Sicherung guter wissenschaftlicher Praxis“ niedergelegt sind, eingehalten.

---

Ort, Datum

---

Florian J. Ritz

**Erstgutachter:** Prof. Dr. Siegfried Schindler

**Zweitgutachter:** Prof. Dr. Richard Göttlich

## Danksagung

Ich möchte mich ganz herzlich bei Prof. Dr. Siegfried Schindler bedanken, dass er mir die Möglichkeit gegeben hat, in seiner Arbeitsgruppe zu promovieren und mich während der gesamten Zeit stets unterstützt hat. Prof. Dr. Richard Göttlich danke ich für das Zweitgutachten dieser Arbeit.

Weiterhin möchte ich mich bei Dr. Jonathan Becker für die regelmäßigen Messungen der Einkristall-Röntgendiffraktometrie und die Strukturlösungen bedanken. Auch danke ich Dr. Christopher Gawlig und Dr. Andreas Miska für die zusätzlichen Messungen der Einkristalle. Besonderer Dank gilt meinem Kollegen Stefan Schaub für die vielen wissenschaftlichen Anregungen, die Unterstützung bei präparativen Techniken und sein langjähriges Mentoring seit Bachelorzeiten.

Ganz herzlich danken möchte ich meinen ehemaligen Kollegen der Arbeitsgruppe Schindler Dr. Tim Brückmann, Chiara Campi, Dr. Christopher Gawlig, Alexander Granichny, Dr. Markus Lerch, Frank Mehlich, Dr. Andreas Miska, Christian Noß, Alexander Petrillo, Dr. Thomas Rotärmel, Stefan Schaub, Lars Schneider, Dr. Pascal Specht, Dr. Fabian Stöhr und Dr. Miriam Wern für das tolle Arbeitsklima und die schöne Zeit im Labor und nach Feierabend. Ebenfalls möchte ich den Studierenden danken, die in Forschungsprojekten und Abschlussarbeiten einen wertvollen Beitrag zur Entstehung dieser Arbeit geleistet haben. Nicht zuletzt gilt mein Dank den Korrekturlesern der Arbeit Dr. Pascal Specht und Dr. Christopher Gawlig.

Meinen früheren Kommilitonen aus dem Chemiestudium, insbesondere Dr. Tim Brückmann, Yannic Decker, Dr. Christopher Gawlig, Dr. Vanessa Linke, Dr. Florian Lotz, Raika Oppermann, Dr. Simon Randau und Michael Waletzko danke ich für die Begleitung auf diesem langen Weg.

Abschließend möchte ich mich besonders bei meiner Familie sowie meiner Partnerin Sarah-Maria bedanken, die mich in den vielen Jahren des Studiums und der gesamten Promotion immer voll unterstützt haben.

*Für Sarah und Aria*

*“A scientist is just a kid who never grew up.”*

– Neil DeGrasse Tyson

## Table of Contents

Abstract .....	1
Zusammenfassung .....	2
1. Introduction .....	3
1.1 Catalysis in Industrial Processes .....	3
1.2 Nickel catalysts in Olefination .....	5
1.3 Metalloproteins as Catalysts in Biological Systems .....	6
1.3.1 Iron-containing Enzymes .....	8
1.3.2 Dioxygen Activation in Iron Enzymes .....	11
1.4 Model Complexes of Iron Proteins and Enzymes .....	14
1.4.1 Macrocyclic Ligands .....	17
2. Research Goals .....	20
3. Syntheses, Structural Characterization, and Kinetic Investigations of Metalla[3]triangulanes: Isoelectronic Nickel(0) and Copper(I) Complexes with Bicyclopropylidene (bcp) and Dicyclopropylacetylene (dcpa) as Ligands.....	22
4. Kinetic investigations of the formation of iron(IV) oxido complexes .....	31
5. References .....	46
5.1 Copyright References.....	50

## Abstract

Catalytic reactions with widely available and low-cost transition metals are among the important building blocks of the modern chemical industry with its thousands of products. Most of these however can be traced back to a limited number of basic reactions. The detailed study of these reactions in fundamental organometallic research is therefore at the beginning of the process chain in order to understand the ideal conditions for the catalytic conversions. Furthermore, an increase in efficiency and cost optimization is always in focus, which can be achieved by cheaper and more efficient catalysts or adapted reaction conditions at low pressures and temperatures. Detailed mechanistic investigations can be carried out, for example, by spectroscopic methods at low temperatures, so that equilibrium constants can be determined for wide temperature ranges and basic reaction parameters and mechanisms can be derived.

In Chapter 3 the reactions of nickel(0) precursors and an isoelectronic copper (I) precursor with novel cyclopropane-containing olefinic and acetylenic ligands were investigated and kinetic measurements via stopped-flow UV-vis spectroscopy were performed at various temperatures. In the mechanistic studies with the ligand bicyclopropylidene (bcp) an associative or associative interchange mechanism with an ordered transition state could be shown as the basis of the conversion. Reactions with the ligand dicyclopropylacetylenes (dcpa) were also performed in comparison and a structural study of the complexes with nickel and copper and description of features of the molecular structures were carried out. The obtained results of the structural analyses were further compared with literature known complexes with other transition metals.

In Chapter 4 the reactivity of several iron(II) complexes with the ligand cyclam and its methylated derivatives, especially tetramethylcyclam (TMC) toward various oxygen species is shown. The successful formations of desired oxido-complexes, which are relevant in multiple enzymatic reactions as key compounds, were also investigated spectroscopically in the low temperature range and mechanistic studies were performed. One example is an iron(II) complex supported by the ligand TMC and a triflate anion in reaction with aqueous hydrogen peroxide. Its possible mechanism based on the measured data is shown with the rate-determining step being the initial addition of H<sub>2</sub>O<sub>2</sub>. Furthermore, complexes of the open-chain and guanidine-based ligand DMEG<sub>3</sub>tren were spectroscopically studied as iron and chromium complexes to obtain a first overview and comparison of different systems and their reactivity.

## Zusammenfassung

Katalytische Reaktionen mit leicht verfügbaren und günstigen Übergangsmetallen zählen zu den wichtigen Bausteinen der modernen Chemieindustrie mit ihren tausenden Produkten. Die meisten davon lassen sich jedoch auf wenige Basisreaktionen zurückführen. Eine detaillierte Untersuchung dieser Reaktionen in metallorganischer Grundlagenforschung steht daher am Anfang der Prozesskette, um die idealen Bedingungen für zukünftige katalytische Umsetzungen zu verstehen. Des Weiteren ist eine Effizienzsteigerung und Kostenoptimierung stets im Fokus, was durch günstigere und effizientere Katalysatoren oder angepasste Reaktionsbedingungen bei geringeren Drücken und Temperaturen erzielt werden kann. Detaillierte mechanistische Untersuchungen können durch spektroskopische Methoden bei tiefen Temperaturen erfolgen, sodass Gleichgewichtskonstanten bestimmt und grundlegende Reaktionsparameter und Mechanismen hergeleitet werden können.

In Kapitel 3 wurden die Reaktionen von Nickel(0)-Vorstufen und einer isoelektronischen Kupfer(I)-Vorstufe mit neuartigen olefinischen und acetylenischen Liganden untersucht und kinetische Messungen via Stopped-Flow-UV-vis-Spektroskopie bei verschiedenen Temperaturen durchgeführt. In den mechanistischen Untersuchungen der Reaktionen mit dem Liganden Bicyclopropyliden (bcp) konnte gezeigt werden, dass ein assoziativer oder assoziativer interchange-Mechanismus mit einem geordneten Übergangszustand der Reaktion zugrundeliegt. Auch die Reaktionen mit dem Liganden Dicyclopropylacetylen (dcpa) wurden vergleichend durchgeführt und eine strukturelle Untersuchung der Komplexe mit Nickel und Kupfer vorgenommen. Die Ergebnisse der Strukturanalysen wurden im Detail mit bereits literaturbekannten Komplexen mit anderen Übergangsmetallen verglichen.

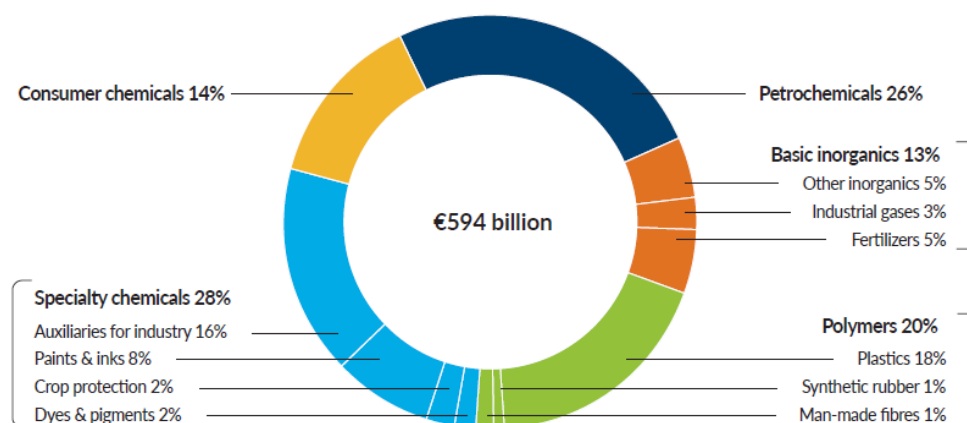
In Kapitel 4 werden die Reaktivitäten mehrerer Eisen(II)-Komplexe mit dem Liganden Tetramethylcyclam (TMC) und seinen Derivaten gegenüber verschiedener Sauerstoffspezies gezeigt. Die erfolgreiche Bildung der gewünschten Oxido-Komplexe, die zentrale Verbindungen in einer Vielzahl enzymatischer Umsetzungen darstellen, wurde im Tieftemperaturbereich spektroskopisch untersucht. Beispielsweise wurden mechanistische Studien an einem Eisen(II)-Komplex mit dem Liganden TMC und Triflatanionen mit wässriger Wasserstoffperoxidlösung durchgeführt. Ein möglicher Mechanismus wurde anhand der Messdaten mit dem geschwindigkeitsbestimmenden Schritt der  $\text{H}_2\text{O}_2$ -Anlagerung aufgezeigt. Des Weiteren wurden Komplexe des offenkettigen und guanidinbasierten Liganden DMEG<sub>3</sub> tren spektroskopisch in Form von Eisen- und Chromkomplexen untersucht, um einen ersten Blick auf den Vergleich von verschiedenen Systemen und deren Reaktivität zu werfen.

# 1. Introduction

## 1.1 Catalysis in Industrial Processes

The impact of catalysis on modern industrial production is essential and cannot be imagined without it. Estimations show that over 90 % of current chemical processes in industry involve catalytic reactions at some stage of their manufacture.<sup>[1]</sup> Global annual sales of manufactured chemicals were about \$900 billion in 2005, and demand continues to grow rapidly, as shown in the 2021 statistics for Europe from Figure 1.<sup>[2]</sup> The individual sectors of chemical production with their shares are also shown. Despite its omnipresence in modern chemistry, the roots of catalysis go back to the dawn of human civilization, even if people did not know the term at that time. The first example of an applied catalytic-technical process is the fermentation of sugar to produce alcoholic beverages such as beer and wine. The actual term *catalysis* was first proposed by Jöns Jakob Berzelius in 1835 and is derived from the two greek words *kata*, meaning down, and *lyein*, meaning loose by which he meant the property to form new compounds which they do not enter- which can be considered a very basic definition to this day.<sup>[3]</sup> After the discovery and the beginnings of the application of catalytic procedures, it took some time before industrial processes were developed on a significant scale.

EU27 chemical sales 2021 (€594 billion)



Source: Cefic Chemdata International

**Figure 1:** Total sales of production sectors of EU 27 chemical industry and their shares in 2021.<sup>[4]</sup>

One of the most notable examples, which is still used on a multiton scale around the world today, is the Haber-Bosch process for the production of ammonia, for which the two German inventors Fritz Haber and Carl Bosch were awarded the Nobel Prize in Chemistry (1918 &

1931).<sup>[5]</sup> The invention of the process made it possible to feed the steadily growing population in the first place, as about 80% of the ammonia obtained is immediately used for fertilizer production. In theory, it is a simple reaction between nitrogen and hydrogen (Scheme 1). At first, the nitrogen is extracted from air in the industrial 3-step process in contact with an iron catalyst, but the entire process was only mechanistically elucidated in the 2000s by Gerhard Ertl (honored with Nobel Prize in Chemistry in 2007).<sup>[6]</sup> The required commercial upscaling posed significant challenges to the inventors at the time due to the high pressures required, which were not yet being used on such a large industrial scale.<sup>[7]</sup>



**Scheme 1.** Partial reaction of the formation of ammonia in the Haber-Bosch Process.

The gaseous reactants are passed over an  $\alpha$ -Fe catalyst (enhanced with oxidic promoters of K, Ca, Al resistant towards hydrogen)<sup>[8]</sup> at pressures of 150–200 bar and reaction temperatures of 400–500 °C, so that approx. 15–20 % ammonia can be obtained and separated from the equilibrium reaction. Current world-scale plants (see Figure 2) have daily capacities of 1200 to 2000 tons and very few by-products, as unreacted gases are recycled and reused as fuels, resulting in an overall yield of 97 %.<sup>[9]</sup>



**Figure 2:** BASF Ammonia Process Plant in Ludwigshafen (Germany) © BASF SE <sup>[10]</sup>.

The demands on the catalyst are high, as shown above, because high reactivities, low aging, especially thermal and pressure stability are required and a high resistance to catalyst poisons (traces of H<sub>2</sub>O, O<sub>2</sub>, CO) is needed.<sup>[8]</sup> Therefore alternative Ruthenium- and Cobalt-based catalysts have also been successfully applied mostly in the last decades to address this problem.<sup>[11]</sup>

In view of the energy transition and the shift away from fossil fuels, alternative processes for ammonia synthesis have been developed in recent decades. Promising examples are electrochemical syntheses that couple electrochemical water splitting with new and improved Haber-Bosch pathways,<sup>[12]</sup> metallocomplex fixation of nitrogen<sup>[13]</sup> or photocatalytic and photoelectrocatalytic coupled methods for “Nitroconversion”.<sup>[14]</sup> As mentioned before, the role of sustainability and the shift to more climate-friendly methods in production are becoming an important task in the development of optimizations for large-scale industrial productions.

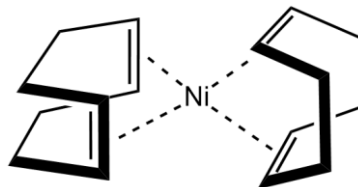
However, ecological and profit-oriented economic aspects are not necessarily in conflict with each other. For example, reducing energy consumption in the light of rising energy costs and producing under mild conditions, would lead to lower greenhouse gas emissions on the one hand, but also reduce costs on the other. In many important reactions and processes transition metals and especially precious metals are used as catalysts.<sup>[15]</sup> Their low natural abundance and the resulting high costs of the platinum group metals are significantly driving the search for cheaper metals with similar reactivities, such as iron, nickel and copper, for example.

### 1.2 Nickel catalysts in Olefination

The catalysis of organic reactions by nickel complexes has a long history, dating back to the widely known studies from Walter Reppe in the 1940s describing a series of impressive transformations including the cyclotetramerization of acetylene to cyclooctatetraene.<sup>[16]</sup> These studies included a description of the involvement of a nickel metallacycle, which is a class of reactive intermediates that plays an essential role in many groups of reactions. In addition to the long history with many significant developments in the field of C-C and C-heteroatom bonding processes, there has been an increase in interest in recent years.<sup>[17]</sup> In particular, first-row transition metals, such as nickel, are of great concern, both in terms of the potential for lower catalyst costs and the exploitation of new reactivity species.<sup>[18]</sup> Soon after the important discoveries from Reppe, an extensive program studying the structure and reactivity of organonickel species was initiated in Mühlheim in the laboratories of Günther Wilke. Many insights into the oligomerization reactions of small molecules such as ethylene and acetylene emerged from his program.<sup>[19]</sup> Their research even led to the formulation of the so called “nickel-effect”, which describes the role of the catalytically active nickel hydride complexes and their influence on the reaction outcome.<sup>[20]</sup>

In general nickel can be utilized in many different reaction types, including cross-coupling reactions of e.g. alkenes and alkynes or phenol derivatives<sup>[21]</sup> and other C-O substrates<sup>[17]</sup>, cycloadditions including [4+2]<sup>[17]</sup> and [2+2+2]<sup>[22]</sup>-type reactions.

The traditionally most studied reactions are the specific olefine dimerizations or oligo- and polymerizations.<sup>[16,19]</sup> Furthermore, in the synthesis of complex molecules (e. g. different alkaloids) these reactions have also been utilized, where the nickel-catalyzed process is a critical step in the overall synthetic route.<sup>[23]</sup>



**Scheme 2:** Structure of Bis(cycloocta-1,5-dien)nickel(0) usually referred as Ni(COD)<sub>2</sub>.

Among these different types of reactions, Ni(COD)<sub>2</sub> (see Scheme 2) and similar complexes are one of the most commonly used and studied catalysts for such reactions, despite their high sensitivity to oxygen.<sup>[24,25]</sup> To circumvent this problem, the complex is used in many conversions as a pre-catalyst and then converted in-situ into less sensitive and more robust catalysts.<sup>[26]</sup> Synthetic routes generally start from a nickel(II) complex that is reduced in a pre-reaction leading to the final Ni(0)-catalyst.<sup>[27]</sup> In current research, nickel compounds (incl. nanoparticles) were also utilized in hydrogenation reactions<sup>[28]</sup> and reductive couplings<sup>[21]</sup> of different substrates e.g. carbonyl, amines etc.<sup>[23]</sup>

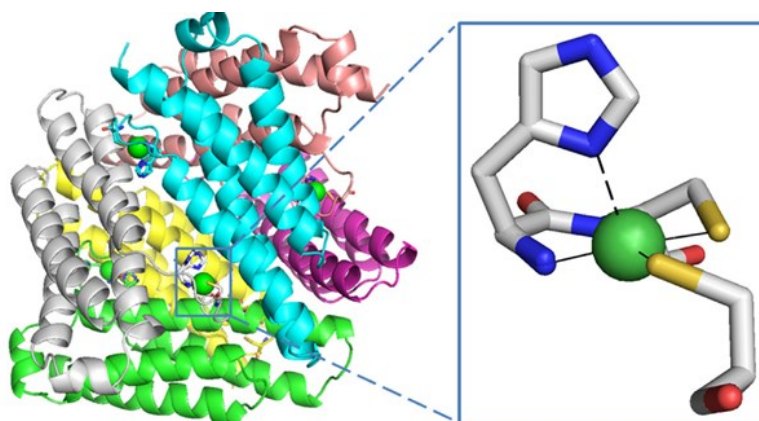
### 1.3 Metalloproteins as Catalysts in Biological Systems

While organometallic catalyses are indispensable in industrial applications, biological systems in the form of metalloproteins have always utilized the catalytic properties of metals or more specifically transition metals. These metalloproteins are key components for living organisms and take part in a variety of different functionalizations as catalysts in biological processes, such as photosynthesis, respiration chain or binding and activation of small molecules such as dioxygen.<sup>[29]</sup> Two prominent examples are the elements iron and copper that are particularly important due to their unique redox properties and bioavailability because of the large natural occurrence in the earth's crust.<sup>[30]</sup> Together with zinc, these two metals are also among the three most commonly found transition metals in the human body.<sup>[29]</sup> The metal ions are generally located in the so-called active centers of enzymes or other metalloproteins where they play a crucial role in many vital processes, especially in the binding and activation of molecular dioxygen and electron transfer reactions.<sup>[31]</sup> In these biological systems, however, the metal ions are not present in the form of oxides, but are instead incorporated typically in

big organic framework consisting of proteins built from amino acids. Transition metals that are present in living organisms are mainly copper, iron, manganese, nickel and zinc.<sup>[29,32]</sup>

In contrast to many other transition metals, the biological relevance of nickel in living organisms interestingly was unknown for a long time and was only confirmed in 1975 by the discovery of nickel in the active site of the enzyme urease in jack beans.<sup>[33]</sup> The absorption measurements performed on the urease showed great similarities to other Ni(II) coordination compounds, so that Dixon *et al.* concluded in their publication that nickel was also an essential transition metal. This is in contrast to the fact that nature typically favors nickel compounds in the conversion of mono-carbon substrates, such as CO, CO<sub>2</sub>, and methyl equivalents, over other transition metals, which played a crucial role, particularly in the early stages of the evolution of life on Earth.<sup>[34]</sup> The current state of research indicates that nickel occurs as an essential element in a total of nine different enzymes in various oxidation states and diverse coordination types.<sup>[35,36]</sup>

The so-called superoxide dismutases (SOD) are an example for oxygen activation enzymes that catalyze the disproportionation of superoxide O<sub>2</sub><sup>-</sup> that can potentially damage the cell to oxygen and peroxide O<sub>2</sub><sup>2-</sup> and therefore prevent oxidative stress.<sup>[37]</sup> The superoxide radical is an inevitable byproduct of aerobic metabolism, and its degradation needs to be addressed by SODs with copper or zinc in the active sites of eukaryotes, including humans.<sup>[38]</sup> In comparison, iron or manganese are mainly found in most bacteria or mitochondria.<sup>[36]</sup>



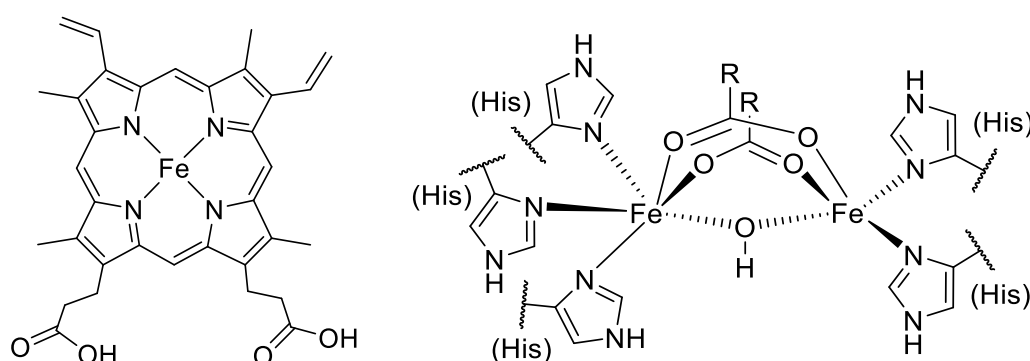
**Figure 3:** NiSOD (superoxide dismutase) structure and active site. The homohexameric structure of NiSOD is shown with each subunit a different color. One active site is shown in the oxidized form, with Ni<sup>3+</sup> (green sphere) coordinated via the amino terminal amine, a backbone amide, two Cys, and an axial His (stick view).<sup>[39]</sup>

Figure 3 (above) shows as a third example a rarely found nickel-containing SOD that is mainly present in prokaryotes, more specifically in *Streptomyces* and *Cyanobacteria*.<sup>[37,40]</sup>

Transition metals are mainly useful in enzymes because of their redox activity, their capability to bind and exchange ligands (especially labile water) and their high charge density, which allows the polarization of substrates as well as the stabilization of intermediates.<sup>[32]</sup> Predominantly, the transition metals occur in mononuclear and dinuclear but also multiple nuclear centers which can be either homonuclear or heteronuclear. Their most frequent ligands are nitrogen, oxygen and sulfur atoms of the polypeptide chain, but cofactors, such as tetrapyrroles, small inorganic compounds such as carbon monoxide and modified amino acids are also used both for metal binding and to exhibit specific metal properties. Other elements such as aluminum are present in large quantities but are not available for biosynthesis due to their natural appearance as inert metal oxides.

### 1.3.1 Iron-containing Enzymes

At approximately 2.5 to 4.0 grams in an average human body, iron is the most abundant essential transition metal and a central component of many proteins and enzymes.<sup>[41]</sup> It normally occurs in the +II, +III, or +IV oxidation states with different types of coordination spheres. Depending on whether an iron metalloprotein contains a heme unit or not they are categorised into two main groups: heme proteins and non-heme proteins (Scheme 3). The heme unit is based on an iron-porphyrin complex, where porphyrin is a macrocyclic N-donor and conjugated type of ligand. Non-heme iron proteins can be further divided into two subcategories: mononuclear non-heme proteins containing only one iron ion in their active sites and dinuclear non-heme proteins, which contain two iron centers linked by an additional bridging ligand, such as a carboxylate, oxido, or hydroxido species.



**Scheme 3:** Schematic active sites of iron heme *b* (e. g. in hemoglobin; left) and of a non-heme iron center (e.g. in hemerythrin; right).

The most well-known iron protein is probably the oxygen carrier protein hemoglobin (Figure 4), which is essential for humans and other mammals because it can reversibly bind molecular

oxygen and, as part of red blood cells is therefore responsible for the distribution of oxygen in the bloodstream. Its quite unique way of quickly binding and releasing molecular oxygen is enhanced by the so-called “cooperative binding effect”, which brings structural changes after oxygen uptake and leads to even higher affinities and a sigmoidal saturation curve.<sup>[29]</sup> Approximately 60 % of the iron stored in the body comes from hemoglobin, another 15-20 % from the storage protein ferritin, and about 10-15 % from myoglobin.<sup>[41]</sup> Only smaller amounts are found in the enzyme systems and in transport proteins, yet they are of enormous importance, as highlighted in the following chapters.

Another iron-based example directly comparable to the mammalian proteins myoglobin and hemoglobin is hemerythrin. It is a non-heme dioxygen transport protein only found in some marine invertebrates species such as sipunculids, annelids, priapulids and brachiopods, which in its most abundant form consists of an octameric O<sub>2</sub> transport protein.<sup>[42]</sup> However, more widespread in biological oxygen transport is the copper-based protein hemocyanin, which is responsible for the characteristic blue blood in many invertebrates caused by the copper (II) oxygenated form.<sup>[43]</sup>

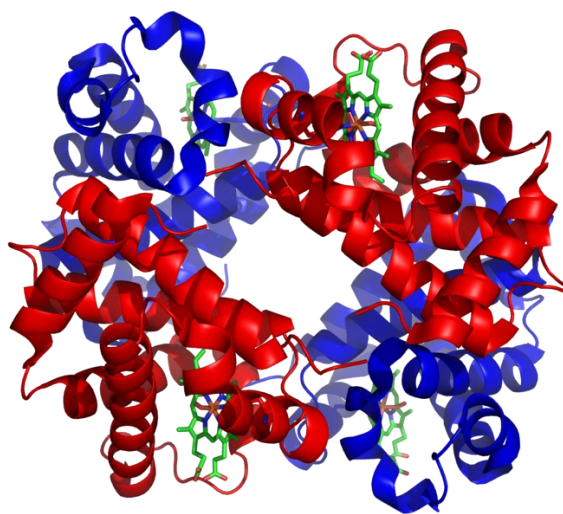


**Figure 4:** Structure of human hemoglobin (heterotetramer) with  $\alpha_1/\alpha_2$  in red and  $\beta_1/\beta_2$  globin subunits in blue. Highlighted iron-containing heme groups in green.<sup>[44]</sup>

In general iron enzymes can act catalytically in many different ways leading to various end products.<sup>[45]</sup> Important examples of these enzymes are performing redox or oxygenation reactions, for example as cytochromes, catalases or peroxidases<sup>[46]</sup> In general, the ability of iron to access multiple redox states, as well as its bioavailability, makes it one of the most common transition metals used for biological O<sub>2</sub> activation and other enzymes.<sup>[47]</sup>

A short overview of different heme and non-heme iron proteins and enzymes and their biological functions are presented in the following Table 1.

**Table 1:** Overview of selected examples of heme and non-heme iron proteins and their basic reactivity and biological function.<sup>[42,48]</sup>

	Reactivity	Biological Function
<b>Heme Iron Proteins</b>		
<i>Hemoglobin</i>	Reversible oxygen binding	Oxygen transport in lungs and blood
<i>Myoglobin</i>	Reversible oxygen binding	Dioxygen storage in muscles
<i>Cytochrome P450</i>	Oxidation C-H sp <sup>3</sup> or sp <sup>2</sup> -bonds	Transformation of a variety of different substrates, including S-, C-H and C=C oxidations
<i>Heme oxygenase</i>	Heme degradation to biliverdin	Degradation of free and toxic heme groups to prevent accumulation
<i>Nitric Oxide Synthase (NOS)</i>	Oxidation of L-arginine	Immediate precursor of NO, an important signalling molecule
<b>Non-Heme Iron Proteins</b>		
<b>Mononuclear</b>		
<i>Rieske dioxygenase</i>	<i>Cis</i> -dihydroxylation	Oxygenation of various substrates, mostly hydroxylation of aromat. rings
<i>Taurine α-KG-dependent dioxygenase (TauD)</i>	Taurine degradation via oxygenation	Conversion of taurine to sulfite and aminoacetaldehyde under α-KG consumption
<i>Bleomycin</i>	H· abstraction	Chemotherapeutic agent to fragment DNA in tumor cells
<b>Dinuclear</b>		
<i>Soluble methane monooxygenase hydroxylase (sMMOH)</i>	Monooxygenation	Hydroxylation of methane in methanogenic bacteria
<i>Ribonucleotide reductase (RNR)</i>	Reduction of ribo- to deoxyribonucleotides	Essential in biosynthesis of DNA
<i>Ferritin</i>	Reversible storage of Fe <sup>3+</sup>	Iron storage in cells
<i>Hemerythrin</i>	Reversible oxygen binding	Oxygen-carrier in marine invertebrates

### 1.3.2 Dioxygen Activation in Iron Enzymes

The research of dioxygen activation started nearly 70 years ago, when two independent publications were reporting the incorporation of O atoms from dioxygen into oxidation products of enzyme-catalyzed conversions in 1955.<sup>[49]</sup> These works stimulated many scientists to investigate the phenomenon of dioxygen activation in nature, resulting in the identification of many enzymes as oxygenases, which use a variety of redox-active centers, both organic and inorganic, as agents to activate O<sub>2</sub> for the transformations of biomolecules and the biosynthesis of natural products.

In oxygen activation and subsequent oxygenation of substrates, one potential pathway is via the coordination at a metal center (active site of an enzyme or an artificial catalyst). The study of the catalytic cycles is therefore crucial to get further insights into the actual activation step.<sup>[50]</sup>

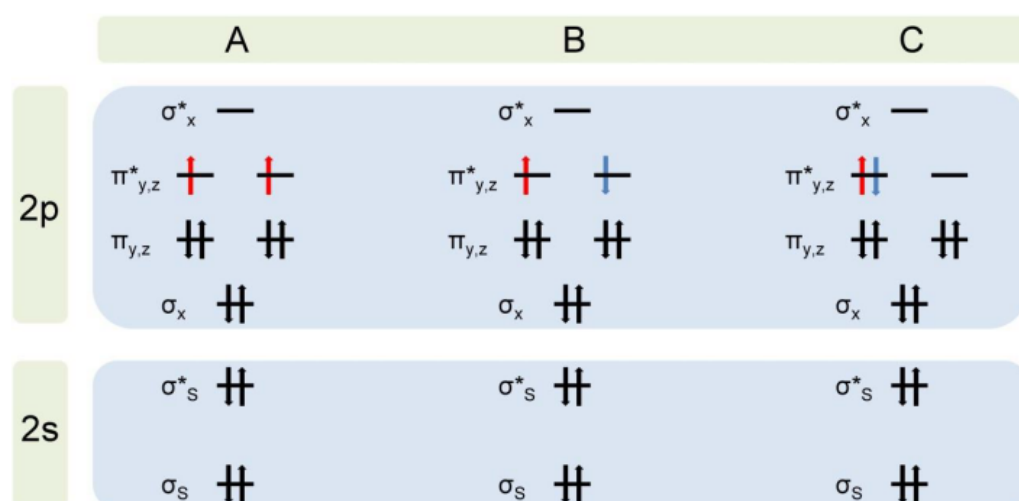


**Figure 5:** Possible electron configurations of the dioxygen molecule: **A** triplet (ground) spin state of dioxygen ( $^3\Sigma_g^-$ ), **B** singlet (excited) spin state with two electrons with different spin in each of the two  $\pi^*$  orbitals ( $^1\Sigma_g^+$ ), **C** singlet (excited) spin state with two coupled electrons in one  $\pi^*$  orbital ( $^1\Delta_g$ ). Redrawn scheme according to reference.<sup>[51]</sup>

In the ground state the dioxygen molecule is a biradical with two unpaired electrons in the  $\pi^*$  molecular orbital and therefore has a triplet spin state (Figure 5). Direct conversions of dioxygen with organic compounds are hindered as most molecules show a closed-shell electronic configuration and therefore a singlet spin state. These reactions are spin-forbidden.<sup>[51]</sup> To perform oxygen inserting reactions dioxygen has to be converted into an activated state. In essence, this means that either a catalyst is needed to carry out oxidation reactions and oxygen activation, i.e. to change the multiplicity of spin of oxygen, and allow the reaction to occur or dioxygen is activated photochemically.<sup>[52]</sup> One goal in metalloenzyme

research is to better understand the structures of the active sites and the intermediates that occur as well as the mechanistic details of oxygen activation, which is realized by suitable model complexes and described in more detail in Chapter 1.4. In Chapter 4, concrete examples of model complexes with central iron ions and their oxygen activation are shown, as well as kinetic studies of the reactions to better understand the mechanisms and individual steps of the enzyme reactions, some of which are complex and difficult to study. The relevance of the subject is well illustrated in the following Figure 7, which shows that very many different reaction types are catalyzed by non-heme iron(IV) oxido complexes, leading to a myriad of new products and reaction pathways. In particular, the aliphatic hydroxylation of unreactive C-H substrates is a prime example of the synthetic relevance of enzymes in biological systems, capable of converting substrates to new functionalized building blocks only by electron and proton transfer. Despite the mild reaction conditions and solvents, the conversions and catalytic activities achieved are very good – conditions that industrial synthesis would like to transfer 1:1, but often fails to do so for various reasons.

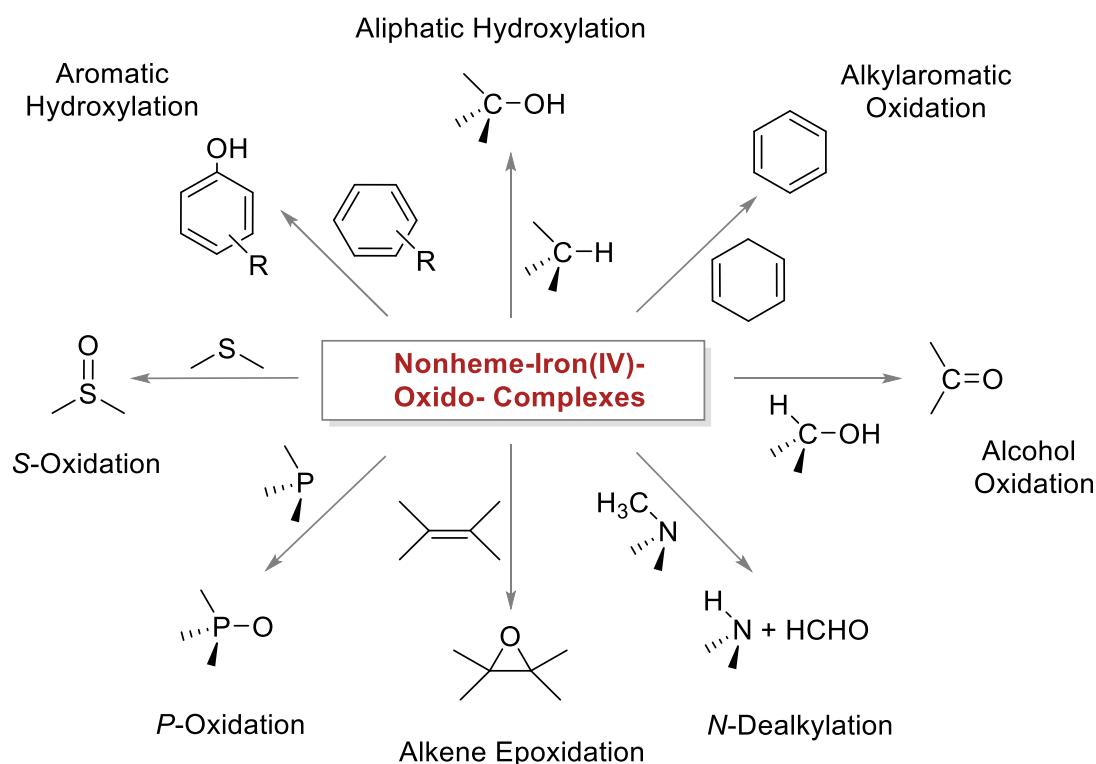


**Figure 6:** Schematic overview of reaction types performed by nonheme-iron(IV) oxido complexes and products.

In oxygen activation chemistry either the oxygen molecule directly or a reduced oxygen equivalent reacts to form a wide variety of complexes (Figure 7) depending on the number of electrons and protons added. This in fact allows various types of interesting metal complexes

with oxygen ligands depending of the oxidation state of the metal cation.<sup>[53]</sup> Most of the research focuses on superoxido, peroxido and oxido complexes, of which there are numerous described representatives with almost all transition metals.<sup>[54]</sup> Chapter 1.4 shows some examples in which model complexes were successfully reacted with oxygen ligands and subsequently oxygen transfer reactions were also successfully carried out. These reactions can in the long run be a real alternative to many current methods of functionalization of hydrocarbon substrates where typically high pressures and/or high temperatures are used to get decent turnover rates for high volume industry processes. Besides the reaction rates especially the chemoselectivity is lacking und mixtures of products are obtained that need a detailed work-up, e.g. by distillation colonnes sperating the fractions on a large scale.

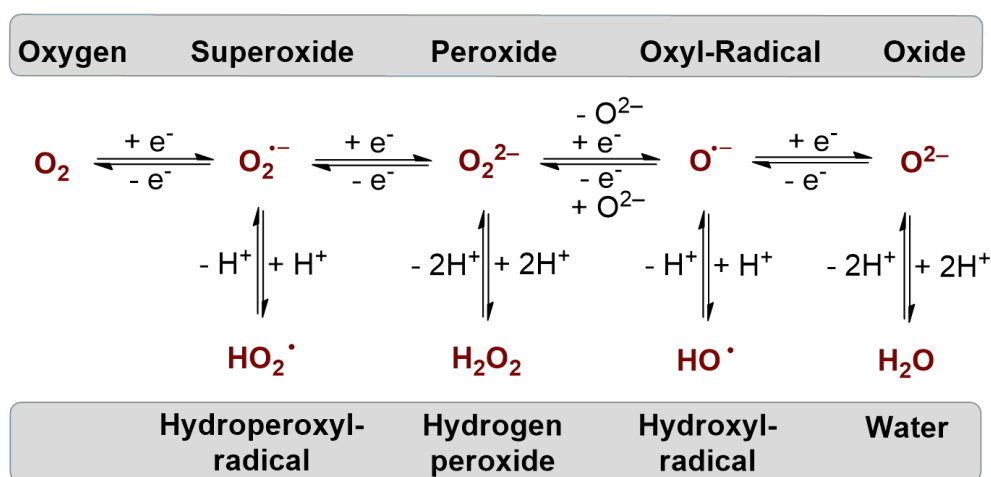


**Figure 7:** Overview of oxygen intermediates formed in biological organisms during the conversion of molecular oxygen to water; addition of electrons in reactions from left to right, addition of protons from top to bottom.

Elemental oxygen is a strong oxidizing agent according to its position in the periodic table resulting in second highest electronegativity of all elements. Moreover,  $O_2$  readily forms highly reactive, partially reduced species catalyzed by transition metals, the neutralization of which requires many biological antioxidants. Under free atmosphere therefore only those aerobic organisms have survived in ancient times which have been able to develop protective mechanisms against oxygen and its very harmful, often radical reduction intermediates. Many substances react strongly exothermic with dioxygen, but often only after activation.<sup>[29]</sup>

The frequently observed, characteristic inhibition of numerous reactions with  $O_2$  can in many cases be explained by the triplet ground state of the  $O_2$  molecule as described in Figure 5. The formal addition of electrons gives the reduced series of oxygen from the oxygen molecule to

the oxide ion, as shown in Figure 7 above. All these oxygen species open further possibilities for synthesis, since a targeted addition of a reduced form of oxygen to transition metals in appropriate oxidation and electronic configuration state leads to a variety of reaction pathways. The most stable form of the final metal complex is the corresponding oxide, but a direct addition of oxides to the precursors is usually not possible because metal oxides do not react further due to their thermodynamic stability. Once metal oxides are formed the central ion of the complex unit is not available for further reactions and no catalytic properties can be observed. The reversibility of the entire reaction is therefore a key prerequisite.

The addition of aqueous solutions of hydrogen peroxide at typical concentrations of 30% (w/w) can lead to peroxido complexes (see for example Figure 8 right), provided that the protons and the aqueous environment do not interfere with the desired reaction. Targeted syntheses to superoxido complexes are also widely-known examples of oxygen activation in nature and bioinorganic research.<sup>[55]</sup> For mononuclear superoxido representatives two different forms of binding are possible: the *end-on* and the *side-on* form of the complex.<sup>[56]</sup> Binuclear complexes open up even further modes of coordination through the bridging superoxido unit.<sup>[57]</sup>

#### 1.4 Model Complexes of Iron Proteins and Enzymes

As mentioned in the previous chapters in-depth research is needed to overcome the challenges in utilizing the reactivities that nature has been using for millions of years in standardized enzymatic reactions. Thus, there is a great interest in bioinorganic chemistry in mimicking the functions and reactivities of natural enzymes with the help of model compounds to achieve a better understanding of the complex mechanisms in biological processes. This understanding can be used for example, to develop new performance materials but also to use accessible systems in chemical research to make reactivity functional for catalytic or synthetic application on an industrial scale. To achieve this greater aim, the often several kilo-Dalton large systems have to be reduced to their basic components: Essentially to the active site with the transition metal in the correct oxidation state and redox properties and a simple ligand system with the appropriate donor atoms and additional co-ligands to enable synthesis and further investigation on a laboratory scale. In case of the heme-containing iron enzymes, macrocyclic ligands with four N-donors are predestined because of the structural similarity to the heme-ligand; for nickel in olefination reactions simple alkenes and alkynes are often used as co-ligands in transformations while the COD (1,5-cyclooctadiene)-ligand is and has been one of the most-used starting systems for the Ni(0) chemistry.<sup>[25]</sup>

In the coordination chemistry of iron there has been much interest especially in the oxygen activation inspired by enzymes in biological systems. The publications and crystallographic characterizations of the first non-heme iron oxido-complexes represent an important milestone in the study of transition metal coordination compounds. In 2000, Borovik *et al.* reported the generation of an iron (III) oxido complex directly from oxygen stabilized by hydrogen bonds.<sup>[58]</sup> As a second example in 2003, Rohde *et al.* succeeded in oxygenating an iron(II) precursor complex with iodoyslbzene in acetonitrile at  $-40\text{ }^{\circ}\text{C}$  and subsequently characterizing it both spectroscopically and crystallographically (Figure 8 left).<sup>[59]</sup>

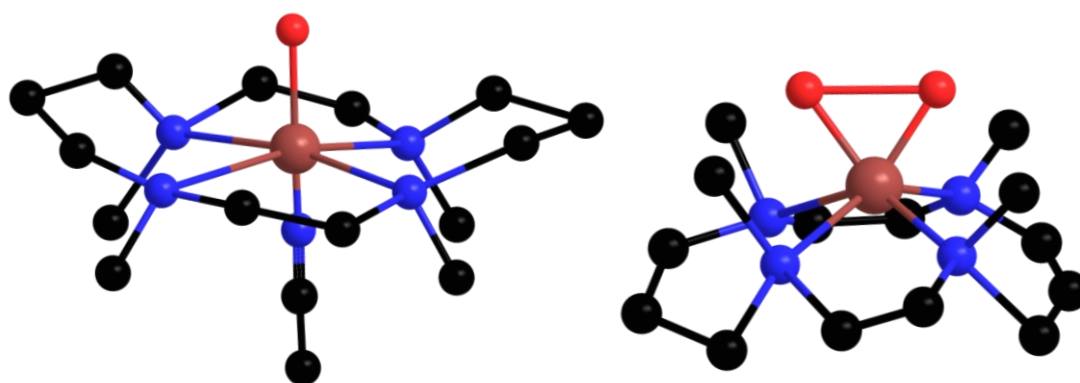


**Figure 8:** Molecular structure of *trans*-[Fe(IV)(O)(TMC)(MeCN)](OTf)<sub>2</sub> (**left**)<sup>[59]</sup> and structure of [Fe(III)(TMC)(OO)]<sup>+</sup> (**right**)<sup>[60]</sup> (cations shown, H atoms omitted) as selected examples of iron complexes with oxygen ligands, redrawn according to references.

From the research group of Nam, Cho *et al.* succeeded in experimentally preparing and studying the mononuclear *peroxido*-complex [Fe(III)(TMC)(O<sub>2</sub>)]<sup>+</sup> by adding hydrogen peroxide and triethylamine to a precursor complex in trifluoroethanol (Figure 8 right).<sup>[60]</sup> Furthermore, the publication described the consecutive protonation to the hydroperoxido complex and the conversion to the already known Fe(IV) oxido analog in a homolytic oxygen cleavage. These mentioned iron species are of high interest since high-valent iron-oxido intermediates play a crucial role in the catalytic cycles of the natural enzymes and the detailed studies and characterisations of the molecular structures provide further insights into their reactivities towards substrates.

Three further examples that are an inspirational basis for the work presented in Chapter 4 (and comparable unpublished work) are depicted under Figure 9 below. Because of the challenges linked to the reactivity of dioxygen, as stated in chapter 1.3.2, in many cases of complexes

with iron(IV)-oxido cores that have been published in coordination chemistry, researchers have involved other oxygen-containing agents besides pure dioxygen.

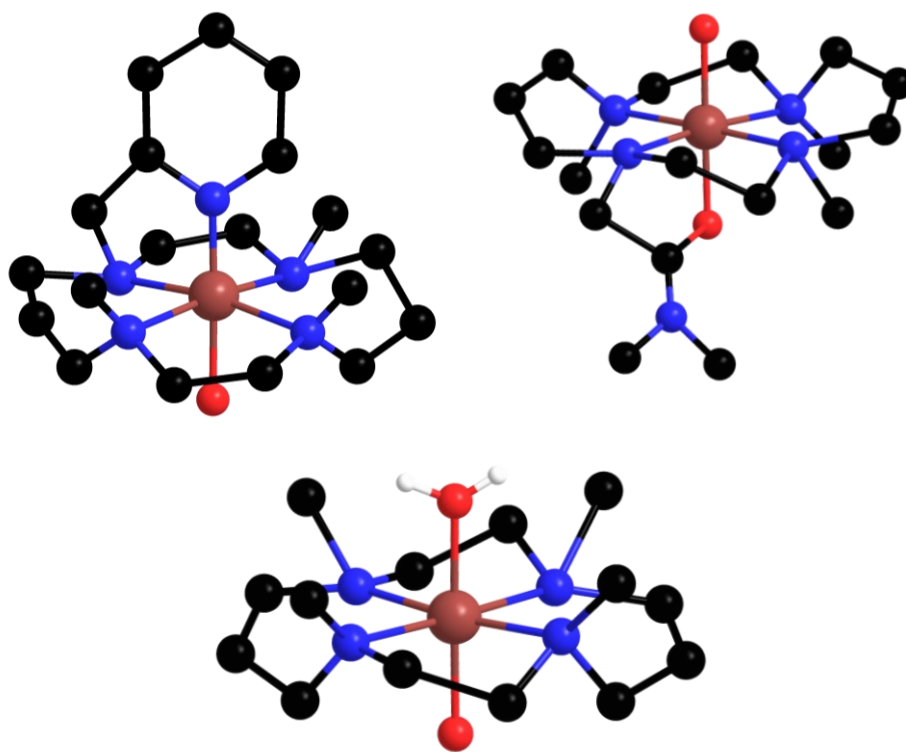


**Figure 9:** Schematic molecule structures of iron(IV)-oxido species (cations shown, most H atoms omitted) with cyclam-based ligands described in 1.4.1 being prominent examples for iron enzyme model complexes:  $[\text{Fe}(\text{O})(\text{TMC-py})](\text{OTf})_2$  (**top left**)<sup>[61]</sup>,  $[\text{Fe}(\text{O})(\text{TMC-CH}_2\text{C=ON}(\text{CH}_3)_2)](\text{OTf})_2$  (**top right**)<sup>[62]</sup>,  $[\text{Fe}(\text{O})(\text{TMC})(\text{H}_2\text{O})](\text{OTf})_2$  (**bottom**)<sup>[63]</sup>, redrawn according to references.

The third depicted example based on iron(II)-TMC, was successfully characterized in the Schindler group in 2018. Schaub *et al.* succeeded in preparing and crystallographically investigating an iron(IV)-aqua-oxido compound by reacting the precursor  $[\text{Fe}(\text{TMC})](\text{SO}_3\text{CF}_3)_2$  with ozone and the subsequent addition of water after successful oxygenation.<sup>[63]</sup> The obtained complex has high biological relevance, since similar oxido-hydroxido derivatives of iron represent a recurring structural motif in catalytic cycles of Rieske-type oxygenases. These iron-dependent non-heme enzymes are capable of catalyzing *cis*-dihydroxylations of substrates, such as naphthalene, in the 1,2-position.<sup>[64]</sup>

Another promising example to mimic the reactivity of the important enzyme soluble methane monooxygenase (sMMO) capable of oxidizing the C-H bond in methane with a direct activation

of molecular oxygen was presented by Ray and coworkers.<sup>[65]</sup> Nevertheless the formation of iron(IV)-oxido complexes from a iron(II) precursor immediately with molecular oxygen still remains a challenge in synthetical coordination chemistry.

### 1.4.1 Macrocyclic Ligands

Macrocyclic ligands have been extensively studied in coordination chemistry. This inhomogenous group of ligands has by definition at least a ring size of nine atoms and more than three donor atoms. They can form stable complexes which is described by the so-called “macrocyclic effect” with high complexation constants in the equilibrium in comparison to open-shell or simple type (single donor) ligands. The effect was described in detail by Cabiness and Margerum in 1969 using the example of copper(II) complexes with the ligand tetra and compared to non-cyclic tetramines.<sup>[66]</sup>

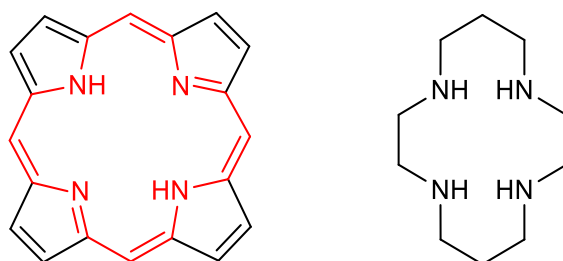
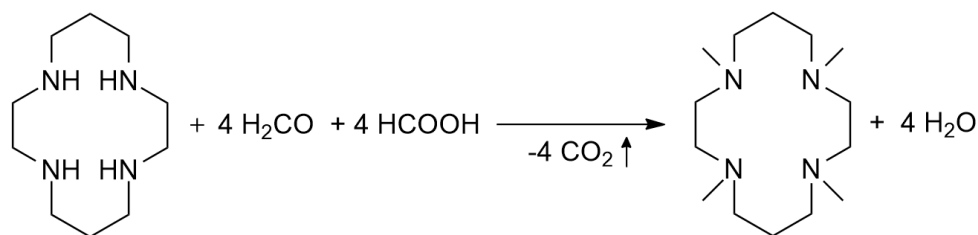


**Figure 10:** The macrocyclic ligands porphyrine and cyclam.

Biological systems use these group of ligands for example in the heme group and (modified) porphyrins. The ligand 1,4,8,11-tetraazacyclotetradecane (cyclam) is among the most studied macrocycles in coordination chemistry as a typical N-donor-ligand. In its classical form it is a 14-atom-containing macrocyclic ring that has four nitrogen donor atoms. Derivatives with smaller ring sizes with 9 to 13 atoms or varying numbers of (mixed) donor atoms, such as sulfur also exist showing a similar structural backbone.<sup>[67]</sup> The N-donors coordinate in an equatorial manner to the central metal ion with bent  $C_2$ - and  $C_3$ -units in the typical coordination sphere. In the axial positions there are in many cases smaller and exchangeable auxiliary-ligands such as water or pendant arms for coordination and the important free coordination site where the desired reactions, e.g. oxygenations, take place.

It was first synthesized by van Alphen in 1937 in a reaction of 1,3-dibromopropane with the primary amine 1,2-diaminoethane, in which the author observed the formation of the

macrocyclic ligand.<sup>[68]</sup> Further, more targeted syntheses have been reported by Stetter and Mayer in 1961, who also showed an IR spectrum of the colorless crystals of the ligand and described the unusual stability of the compound compared to other amines.<sup>[69]</sup> Over the past few decades, coordination compounds with cyclam have been synthesized and characterized with almost all transition metals. Examples include complexes with iron, ruthenium, nickel, manganese, copper, and cobalt as the respective central ions.<sup>[70]</sup> In the following decades, the basic ligand scaffold was further modified in various ways as mentioned in the following: The most straightforward approach is completely substituting the secondary amine functions with the contained protons by methyl groups or by adding more arms to extend the donor properties. The main goals of these modifications were the enhanced ability to stabilize high-valent oxido complexes and the higher stability towards intramolecular oxidation of the ligand, which is a typical problem of these reaction types and which can be achieved by a higher degree of substitution of the protons in general. Especially the amine protons are replaced by chemically more stable groups like methyl or trifluoromethyl to enhance chemical inertness.<sup>[55]</sup>



**Scheme 4:** Schematic reaction of cyclam to tetramethylcyclam.

In this regard, the N-alkylated derivatives of cyclam, which exist in many variants, are of great relevance in the synthesis of complexes with transition metals of all kinds. In particular, the per-methylated derivative tetramethylcyclam (TMC) depicted in Scheme 4 is of interest because it is known from coordination chemistry research that it is able to stabilize high oxidation states of transition metals. It is therefore well suitable to form complexes with oxygen ligands without having the previously mentioned interfering factors. The TMC ligand, which also was utilized in the iron complexes in chapter 4 is typically prepared in a one-step Eschweiler-Clarke reaction from cyclam, which represents a relatively simple synthetic route for the per-methylation of amine functions (see Scheme 4).<sup>[71]</sup> By selective substitution at one or more positions in the molecule, further ligand functions can be attached in the form of nitrogen, oxygen or sulfur donors.<sup>[61,72]</sup> As a consequence, the novel cyclam derivatives are able to coordinate fivefold or even sixfold to the central atoms, leaving less coordination space for undesired side reactions. Another advantage in the coordination of heteroleptic ligands is

that they are more similar to biological systems with amino acid residues that coordinate differently, making them more suitable for model complexes of enzymes.<sup>[62]</sup> However, these more sophisticated derivatives with non-symmetric substitution patterns require more complex reactions with the use of a series of targeted protection and deprotection steps.

In current research also dual-core complexes based on cyclam-moieties have been successfully synthesized to mimic enzymes with bimetallic active centres containing for example iron, copper or nickel ions and a second stabilizing or redox-active metal.<sup>[73]</sup> These ligands typically feature a macrocyclic and an open-shell unit for complexation of two independent metal ions as they are often preferring certain coordination geometries, that can be used for differentiation.<sup>[74]</sup> Similar complexes have also been reported in the oxygen activation. In contrast to the numerous reports of biomimetic synthetic dinuclear complexes involving homo-metallic dioxygen cores, reports on mixed-metal  $[M-O_2-M']^{n+}$  cores are relatively rare, presumably because of intrinsic challenges associated with their preparation such as the numerous possible combinations of the involved metal ions by the methods usually used to obtain their symmetric analogues. Consequently, the synthetic benefit tends to be limited to niche areas although oxygenations have been successfully reported in the past.

## 2. Research Goals

The activation of small molecules such as dioxygen plays a crucial role in many transformations in biological systems but its further application is of particular interest for catalytic reactions in the chemical industry. In this work, therefore, the underlying reactions and reactive intermediates were investigated, which may represent a first cornerstone for the actual subsequent application in catalyses.

As described in the introductory part, organometallic nickel complexes play an important role in a variety of catalytic reactions. In the Schindler group, several nickel-olefin complexes were investigated in previous research, in particular for their capabilities to activate carbon dioxide.<sup>[75]</sup> The resulting complexes of the nickel(0)-based research are presented in chapter 3 and show interesting structural features with unsaturated ligands containing cyclopropanyl-units.<sup>[76]</sup> A starting point of the synthetic work was the reaction of the sensitive precursor complexes with olefinic and acetylenic ligands provided by the former group of Prof. Armin de Meijere. In a first step these reactions were carried out under conditions based on literature known conversions with other transition metals to prove the principle of the formation of the metallacycles with nickel and the unsaturated ligands. The second objective was the structural investigation after the successful formation of the desired complexes with bicyclopropylidene (bcp) and dicyclopropylacetylene (dcpa) as ligands. For these characterisations suitable single crystals were obtained from the saturated solutions after the reactions and storage for days or weeks at low temperatures (ca.  $-80\text{ }^{\circ}\text{C}$ ). After the measurements of the complexes the bond lengths and angles of the coordinating units were compared to similar literature examples. In a second step the formation kinetics were monitored via stopped-flow spectroscopy at low temperatures to get a detailed insight into the complex-forming kinetics and some basic reaction parameters. In a final step, comparisons were also made with the isoelectronic copper(I) complex with dcpa.

Especially the activation of unreactive hydrocarbons and its hydroxylation by iron-containing catalysts and oxygen, as readily performed in many enzymes, is a promising field of research to move away from typical industrial processes to milder conditions. These typically require lower temperatures and pressures, and in many cases are more selective, in addition to producing even fewer byproducts, leading to an overall reduction in cost. However, the replacement of classical industrial processes still requires a lot of further development to make modern catalysts competitive. This is especially true for broad availability for industrially relevant reactions or for catalyst-specific properties such as turnover or reaction rates or (chemo)selectivities. The goal of this work was to investigate the underlying basis reactions

and their kinetics and perform structural investigations. Hence, the detailed results of the research conducted here can form the foundations for more sophisticated research in the future for commercial applications in catalysis.

Research on iron(II) complexes presented in chapter 4 has therefore focused on the synthesis of intermediates and their investigations at room temperature and below, as well as at normal pressure under standard laboratory conditions. In order to perform targeted oxygenations, most reactions and syntheses were carried out under inert conditions, either under Schlenk conditions or in a glove box. At the initial phase of the research work, suitable complex systems were screened from the literature to be able to activate oxygen or reduced equivalents. Precursor complexes were synthesized based on literature-known and well-established systems. The first goal was to reproduce and increase the reactivities and in a second step to modify and optimize the complexes in their ligand properties. In order to track the reactivities the oxygenation reactions were monitored via spectroscopic UV/vis-methods and for further analyses via stopped-flow spectroscopy under low temperature conditions down to circa  $-80\text{ }^{\circ}\text{C}$  in solution. Macrocyclic ligands like cyclam and its methylated derivatives (e. g. TMC) are known for their stability in oxygenation chemistry with many published examples as mentioned before and therefore were a promising starting point. Open-shell ligands like TMG<sub>3</sub>tren bearing a tris(2-aminoethyl)amine base unit and guanidine residues were also investigated since the copper(I) complexes of the respective ligand are also known for their facile oxygen activation. The spectroscopic methods already mentioned were selected depending on the sensitivity of the complexes to oxygen and temperature. In general, the oxygenating agents used for this type of reactions in the present work and further research projects were dioxygen, but also generated ozone, aqueous solutions of hydrogen peroxide, metal salts of superoxide and ozonide.

---

### 3. Syntheses, Structural Characterization, and Kinetic Investigations of Metalla[3]triangulanes: Isoelectronic Nickel(0) and Copper(I) Complexes with Bicyclopropylidene (bcp) and Dicyclopropylacetylene (dcpa) as Ligands

This work has been published in

*European Journal of Organic Chemistry*

Florian J. Ritz, Lars Valentin, Anja Henss, Christian Würtele, Olaf Walter,  
Sergei I. Kozhushkov, Armin de Meijere, Siegfried Schindler

*Eur. J. Org. Chem.*, **2021**, 12, 1864 – 1870.

[doi.org/10.1002/ejoc.202100045](https://doi.org/10.1002/ejoc.202100045)

**Cover Feature:**

*A. de Meijere, S. Schindler et al.*

Syntheses, Structural Characterization and Kinetic Investigations of Metalla[3]triangulanes:  
Isoelectronic Nickel(0) and Copper(I) Complexes with bcp and dcpa as Ligands

**Building  
Blocks**

**Cu**

**Ni**

**bcp**

**Related  
Molecules**

11/2021

WILEY-VCH



# Syntheses, Structural Characterization, and Kinetic Investigations of Metalla[3]triangulanes: Isoelectronic Nickel(0) and Copper(I) Complexes with Bicyclopropylidene (bcp) and Dicyclopropylacetylene (dcpa) as Ligands

Florian J. Ritz,<sup>[a]</sup> Lars Valentin,<sup>[a]</sup> Anja Henss,<sup>[a]</sup> Christian Würtele,<sup>[a]</sup> Olaf Walter,<sup>[b]</sup> Sergei I. Kozhushkov,<sup>[c]</sup> Armin de Meijere,<sup>\*[c]</sup> and Siegfried Schindler<sup>\*[a]</sup>

The kinetics of the reactions between [Ni(bipy)(COD)] and bicyclopropylidene (bcp), dicyclopropylacetylene (dcpa) and 1,4-dimethoxy-2-butyne (dmbu) were investigated using stopped-flow techniques. Similar to previous studies the results support an associative mechanism (activation parameters for bcp:  $\Delta H^\ddagger = 46 \pm 2 \text{ kJ} \cdot \text{mol}^{-1}$  and  $\Delta S^\ddagger = -69 \pm 8 \text{ J} \cdot \text{mol}^{-1} \cdot \text{K}^{-1}$ ) and therefore allowed to postulate a more general reaction mechanism for the reaction pathway. The products, the

nickel(0) complexes [Ni(bipy)(bcp)] and [Ni(bipy)(dcpa)], could be structurally characterized and the molecular structures are presented. In addition, the corresponding copper(I) complexes [Cu(bipy)(bcp)]PF<sub>6</sub> and [Cu(bipy)(dcpa)]PF<sub>6</sub> were also structurally characterized and their reactivity towards dioxygen was investigated. A detailed discussion of the structural properties and comparisons to similar literature-known olefinic complexes with transition metals are presented.

## Introduction

As has been stated before,<sup>[1]</sup> transition metal-catalyzed cocyclizations, which are formal cycloaddition reactions, of alkenes and alkynes as well as other unsaturated building blocks, are outstanding examples for synthetic efficiency. These reactions are highly atom economical and use simple starting materials under mild conditions to form complex cyclic and oligocyclic compounds. Since the synthesis of bicyclopropylidene (bcp, **1**, Scheme 1) has been reported and optimized,<sup>[2,3]</sup> this alkene as well as its derivatives became versatile C<sub>6</sub> building blocks for organic synthesis.<sup>[4,5,6]</sup> For example, methylenecyclopropane, especially **1** and its derivatives, are predestined for the

formation of new cyclopropyl group-containing compounds.<sup>[7]</sup> Alkene **1** can undergo cocyclizations under palladium, nickel and cobalt catalysis.<sup>[8]</sup> However, despite the fundamental interest in the mechanism of these reactions, so far only metalla-[3]triangulanes **1-Ti**, **1-Co** and **1-Pt**, i.e. transition metal complexes of titanium(II),<sup>[9]</sup> cobalt(I)<sup>[9,10]</sup> and platinum(0),<sup>[11,12]</sup> respectively (Scheme 1) with **1** as a ligand have been isolated and structurally characterized, yet little is known about the mechanism of the formation of these complexes.

On the other hand, the twofold cyclopropyl-substituted alkyne, dicyclopropylacetylene (dcpa, **2**, Scheme 1), attracted our attention as an interesting building block and versatile precursor as well. Synthesis of the hydrocarbon **2** was first

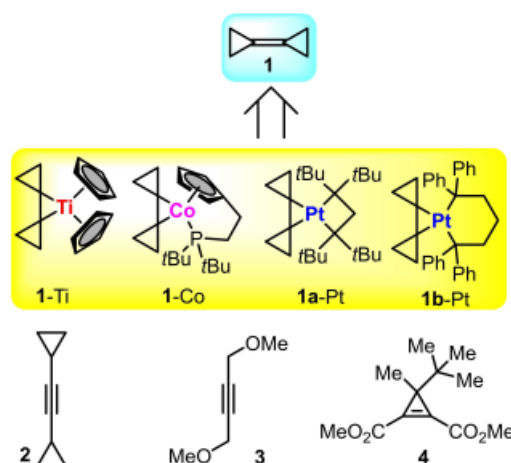
[a] F. J. Ritz, Dr. L. Valentin, Dr. A. Henss, Dr. C. Würtele, Prof. Dr. S. Schindler  
Institut für Anorganische und Analytische Chemie  
Justus-Liebig-Universität Gießen  
Heinrich-Buff-Ring 17, 35392 Gießen, Germany  
E-mail: Siegfried.Schindler@ac.jug.de  
<https://www.uni-giessen.de/fbz/fb08/Inst/iaac/schindler>

[b] Dr. O. Walter  
European Commission, DG Joint Research Centre,  
Directorate G – Nuclear Safety and Security G.I.S – Advanced Nuclear  
Knowledge  
P. O. Box 2340, 76125 Karlsruhe, Germany

[c] Dr. S. I. Kozhushkov, Prof. Dr. A. de Meijere  
Institut für Organische und Biomolekulare Chemie  
Georg-August-Universität Göttingen  
Tammannstraße 2, 37077 Göttingen, Germany  
E-mail: ameijer1@gwdg.de  
<http://www.adm.chemie.uni-goettingen.de>

Supporting information for this article is available on the WWW under  
<https://doi.org/10.1002/ejoc.202100045>

© 2021 The Authors. European Journal of Organic Chemistry published by Wiley-VCH GmbH. This is an open access article under the terms of the Creative Commons Attribution Non-Commercial NoDerivs License, which permits use and distribution in any medium, provided the original work is properly cited, the use is non-commercial and no modifications or adaptations are made.



Scheme 1. Bicyclopropylidene (**1**) and two alkynes **2** and **3**, employed as ligands in the current work in comparison to dimethyl 3-methyl-3-tert-butylcycloprop-1-ene-1,2-dicarboxylate (**4**).<sup>[13]</sup>

reported in 1970<sup>[14]</sup> and has been improved more recently.<sup>[15–17]</sup> For example, this compound was applied in the preparation of perspirocyclopropanated cyclic oligoacetylenes<sup>[17]</sup> and other compounds with several cyclopropane moieties on adjacent carbon atoms under appropriate conditions.<sup>[18]</sup> Interestingly, cobalt(I)-catalyzed *Z*-regioselective hydrosilylation of **2** proceeds with retention of both cyclopropanes and affords (dicyclopropylvinyl)silanes which are valuable starting materials in organic syntheses.<sup>[19]</sup> To the best of our knowledge and in line with the Cambridge Structural Database (CSD), no crystal structures of metal complexes with **2** as a ligand have been reported so far.

With regard to the interesting structural properties of transition metal complexes of **1** and **2** and their potential catalytic activities, the formation of nickel(0) and copper(I) complexes with these ligands were studied.

## Results and Discussion

### Synthesis and Structural Characterization of Nickel(0) Complexes [Ni(bipy)(bcp)] (1-Ni) and [Ni(bipy)(dcpa)] (2-Ni)

The complexes **1-Ni** and **2-Ni** were obtained by mixing [Ni(bipy)(COD)] (**5**) with an excess of the respective ligand **1** or **2** in either diethyl ether or tetrahydrofuran.<sup>[20,21]</sup> While easily prepared, the two complexes are extremely sensitive towards dioxygen, which therefore precluded their full characterization. However, it was possible to crystallize both **1-Ni** and **2-Ni**, and

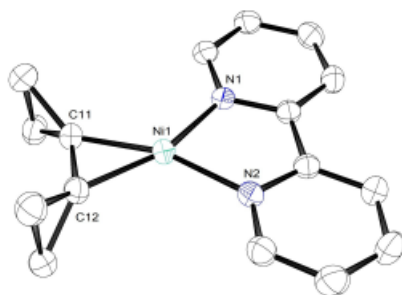


Figure 1. ORTEP plot of the complex **1-Ni**. Ellipsoids at 50% probability, hydrogen atoms omitted for clarity.

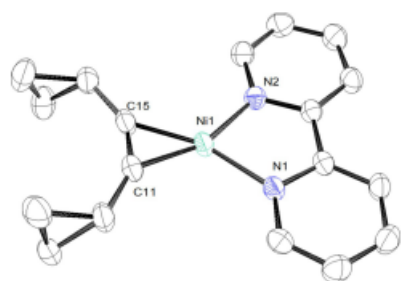


Figure 2. ORTEP plot of complex **2-Ni**. Ellipsoids at 50% probability, hydrogen atoms omitted for clarity.

their molecular structures are presented in Figure 1 and Figure 2 (crystallographic data are reported in the Supporting Information).

The green colored complex **1-Ni** shows the typical  $\eta^2$ -binding motif of the alkene, and the trigonal coordination geometry characteristic for a metalla[3]triangulane. In addition, a severe bending of the cyclopropane moieties is revealed in the molecular structure. This is a consequence of the strong back-bonding effect<sup>[9,10]</sup> which also leads to a remarkably longer double bond [1.422(4) Å, 9.0%] of the coordinated ligand (Table 1) in comparison to the free molecule of **1** [1.304(2) Å].<sup>[4,22]</sup> Interestingly, the elongation of the C=C distances in 1,5-cyclooctadiene [1.340(3) Å],<sup>[23]</sup> ethylene [1.337(2) Å], butadiene [1.342(1) Å],<sup>[24]</sup> and styrene [1.325(2) Å]<sup>[25]</sup> upon formation of similar nickel complexes is equal to  $\Delta = 0.053$ ,<sup>[26]</sup> 0.055,<sup>[27]</sup> 0.073,<sup>[28]</sup> and 0.118 Å.<sup>[27]</sup> Notably, the latter value is the same as  $\Delta = 0.118$  Å caused by effect of spirocyclopropanes in **1-Ni**. Comparable lengths of the double bonds of 1.441(8) Å<sup>[11]</sup> and 1.427(3) Å<sup>[12]</sup> were observed for the previously reported platinum(0) complexes **1a-Pt** and **1b-Pt**, respectively. In addition, the proximal bonds of the ring spiro-annulated to the nickelacyclopropane moiety (average 1.496 Å) are slightly shortened as compared to the distal C–C bonds (average 1.520 Å); the latter, however, are shortened in comparison to the normal C–C bond (1.544 Å). This can be attributed to the hybridization change of the spiro carbon atoms from  $sp^2$  to  $sp^{3[15,17]}$  and is a common phenomenon in triangulane structural features.<sup>[6]</sup> The nickel-carbon distances in the complex **1-Ni** are 1.883(2) Å and 1.895(2) Å. The average Ni–C distance of 1.889 Å in spirocyclopropanated complex **1-Ni** is shorter than the distances in analogous three-coordinate Ni complexes with ordinary alkenes (1.921–2.064 Å),<sup>[26–29]</sup> probably due to the enhanced contribution of  $\pi$  back-donation. Also, the angle C–Ni–C in the nickelacyclopropane moiety of **1-Ni** (44.2°) turned out to be the largest one in comparison with the sequence of complexes with cyclooctadiene (39.6°),<sup>[26]</sup> ethylene (42.4°)<sup>[27]</sup> and styrene (43.4°).<sup>[27]</sup>

Some differences in the bond lengths of spirocyclopropane-annulated **1-Ni** in comparison to the rather similarly strained cyclopropanefused **4-Ni** are noted.<sup>[13]</sup> The cyclopropene ligand **4** is substituted with two methoxycarbonyl groups, a methyl and a *tert*-butyl substituent (Scheme 1). The nickelabicyclobutane moiety in **4-Ni** has slightly elongated nickel- $C_{olefin}$  bond lengths with 1.897(5) Å. However, the former olefinic C–C bond length is 1.437(9) Å and even remarkably longer than the one in **1-Ni**,

Compound <sup>d</sup>	C=C	C–C <sub>dist.</sub>	C–C <sub>vic.</sub>	C–Met	Ref.
<b>1-Co</b>	1.401(5)	1.499(12)	1.482(5)	1.960(4)	[9]
<b>1a-Pt</b>	1.441(8)	1.504(7)	1.482(5)	2.052(3)	[11]
<b>1b-Pt</b>	1.427(3)	1.518(3)	1.488(4)	2.077(3)	[12]
				2.050(3)	
<b>1-Ni</b>	1.422(4)	1.524(4)	1.496(4)	1.883(2)	This work
		1.515(4)		1.895(2)	
<b>1-Cu</b>	1.364(3)	1.531(2)	1.476(2)	1.961(2)	This work

[a] Not reported for **1-Ti**.

being in the range of typical  $sp^3-sp^3$  carbon-carbon bond lengths. A strong bending of the residual groups is again observable in their structure.

The binding motif in **2-Ni** is similar to that in complex **1-Ni** with regard to the trigonal-planar coordination geometry and the strong outward bending of the two cyclopropyl rings.<sup>[20]</sup> The internal C–C bond distance with 1.283(3) Å is again significantly longer than the C≡C triple bond of the free alkyne molecule [1.197(3) Å, calculated data:<sup>[30]</sup>  $\Delta=0.086$  Å], and the metal-carbon bond distances are 1.851(3) Å and 1.854(3) Å. Similar values have been reported previously by J. J. Eisch et al. for the elongated C≡C triple bond in the corresponding complex of diphenylacetylene [1.294(4) Å<sup>[31]</sup> vs. 1.206(2) Å in the parent tolan;<sup>[32]</sup>  $\Delta=0.088$  Å]. The metal-carbon bond lengths in **2-Ni** differ from 1.846(6) Å to 1.859(9) Å for the two independent molecules of the complex in the asymmetric cell. The angles C–Ni–C in the nickelacyclopropene moiety of **2-Ni** (40.5°) and of diphenylacetylene-derived complex (40.8°)<sup>[31]</sup> are of virtually the same value.

**Molecular structures of the Cu(I) complexes with the unsaturated ligands 1 and 2.** Since only a few examples of structurally characterized metal complexes with the ligands **1** and **2** have been reported so far, it looked promising to also prepare the corresponding Cu(I) complexes and analyze the structural and kinetic similarities and differences. Both complexes [Cu(bipy)(bcp)]PF<sub>6</sub> (**1-Cu**) and [Cu(bipy)(dcpa)]PF<sub>6</sub> (**2-Cu**) were obtained by mixing the copper(I) salt [Cu(MeCN)<sub>4</sub>]PF<sub>6</sub> with 2,2'-bipyridine and an excess of either the alkene **1** or the alkyne **2**. Similar to the nickel compounds described above, it was not possible to fully characterize these complexes. However, after subsequent crystallization efforts, the molecular structures could be solved;<sup>[20]</sup> the cations of both complexes **1-Cu** and **2-Cu** are presented in Figure 3. It is obvious that the structures of both complexes are very similar to their nickel analogues. The basic structural motifs are the same, e.g. the nearly trigonal planar coordination geometry and the outward bending of the spirocyclopropane moieties. Due to the high symmetry of the structure of the copper alkene complex **1-Cu**, the pairs of two adjacent Cu–N [1.976(2) Å] and Cu–C [1.961(2) Å] bonds are of the same length.

The C=C double bond in **1-Cu** with a length of 1.364(3) Å is elongated (4.5%) in comparison to that in the free ligand [1.304(2) Å]. This is due to the same effect as discussed above,

the change of hybridization from  $sp^2$  to  $sp^3$ . For comparison, in the previously discussed complexes **1-Co**,<sup>[9]</sup> **1-Pt**<sup>[11,12]</sup> and **1-Ni** (this work) the C=C bonds varied from 1.401(5) to 1.441(8) Å (Table 1). This nicely shows the differences in the mode of coordination of three different metal centers resulting in different elongations of the double bonds. In a similar copper (I)-ethylene complex supported by a neutral amino ligand, the C=C bond length is 1.359(7) Å.<sup>[33]</sup> This is only slightly longer than in a free ethylene molecule [1.337(2) Å], but being close to those in the complex **1-Cu** reported here. Therefore, compound **1-Cu** can be less well regarded as a member of the family of metalla[3]triangulanes. On the other hand, the difference between the elongated distal [1.531(2) Å] and the shortened vicinal [1.476(2) Å] bonds is the biggest in this series and not in line with the geometries of cyclopropanes with electron acceptors.<sup>[34]</sup> The metal-ethylene bonding is in a similar dimension and shows a Cu–C bond length of 1.961(2) Å.

In complex **2-Cu** comparable structural properties can be found, and the ligand again shows a strong outward bending of the cyclopropane rings (Figure 3). The coordinated C–C triple bond is slightly longer (3.1%) than in the free alkyne [1.234(5) vs. 1.197(3) Å].<sup>[30]</sup> This is in the same dimension as in a copper-acetylene complex with a C–C triple bond of 1.188(11) vs. 1.204(3) Å<sup>[33]</sup> showing a slightly shorter bond length in contrast to the previously observed trend.<sup>[34]</sup> In regard to the Cu–C bond lengths of 1.951(4) and 1.962(4) Å, the values are nearly identical with those in the copper complex of **1** and the known copper-acetylene complex.<sup>[33]</sup> In general, the trend of the structures reported here and those of similar complexes can be summarized with the fact, that copper(I), in sharp contrast to nickel and other metal ions, does not exhibit strong  $\pi$ -backbonding interactions leading to shorter metal-carbon and remarkably longer carbon-carbon double and triple bonds in the metal-coordinated molecules.

#### Kinetic Investigation of the Formation of the Ni(0) Complexes

The reactions of [Ni(bipy)(COD) (**5**) with **1** and **2** can be monitored spectroscopically to obtain a better mechanistic understanding with the stopped-flow technique, as has been described previously in detail for the reactions of **5** with benzaldehyde, propionaldehyde and isoprene.<sup>[35]</sup> Due to the

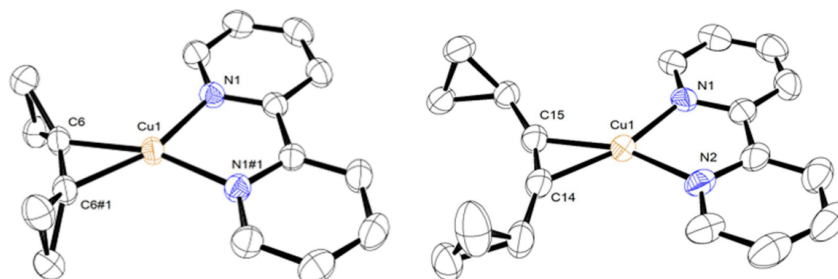
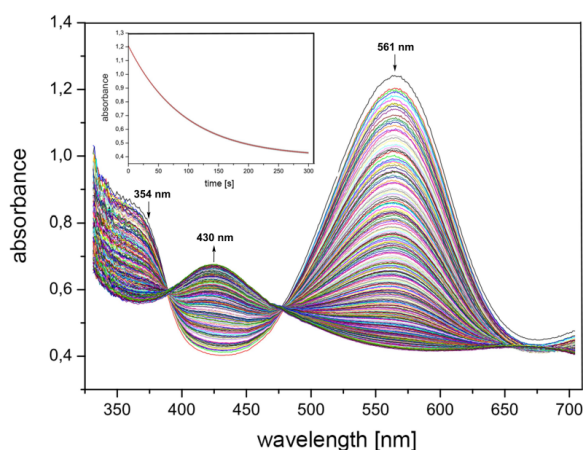


Figure 3. ORTEP plots of complexes **1-Cu** (left) and **2-Cu** (right). Ellipsoids at 50% probability, hydrogen atoms and counter anions omitted for clarity.

extreme sensitivity of the Ni(0) complexes towards dioxygen, these reactions cannot easily be monitored.<sup>[36]</sup> However, by using air-tight glass syringes filled in a glove box, prior to the measurements and special reaction conditions to suppress side reactions this problem could be overcome.<sup>[21]</sup> Time-resolved spectra for the reaction of **5** with **1** are presented in Figure 4.

In case of complex 1-Ni, the decrease of the absorbance maxima at 354 and 561 nm are characteristic for the disappearance of the precursor complex [Ni(bipy)(COD)] (**5**), whereas the increase of the absorbance at 430 nm indicates the formation



**Figure 4.** Time-resolved UV-vis spectra of the reaction of **5** with ligand **1** in THF; concentrations: [5] = 0.25 mM, [1] = 30 mM, T = -20.2 °C, t = 299.5 s, Δt = 1 s. Inset: Absorbance vs. time trace at 561 nm with single one-exponential fit (red).

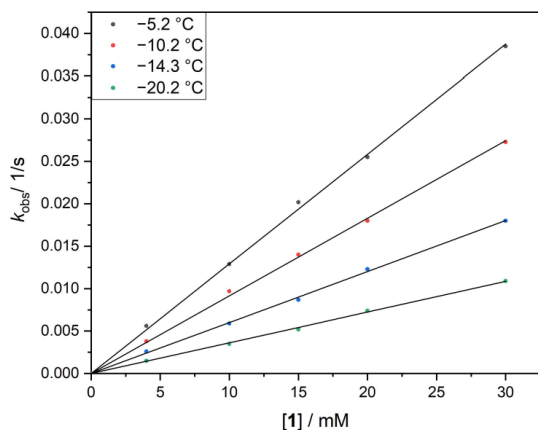


**Figure 5.** Plot of  $k_{\text{obs}}$  vs. concentration of 1-Ni at four temperatures for second-order rate constant determination with linear fits (black lines).

of 1-Ni. Isosbestic points at 390 nm and 478 nm disclose that no spectroscopically observable intermediates are formed. The kinetic measurements were carried out under pseudo first-order conditions, which were ensured by an excess of ligand **1**. The plot of absorbance vs. time at 561 nm was fitted to a single one-exponential function which allowed the determination of the pseudo first-order rate constants  $k_{\text{obs}}$  (see inset in Figure 4) leading to the simple rate equation of  $v = k_{\text{obs}} \times [5]$ . All reactions were measured at four different temperatures with five different ligand concentrations. From a plot of  $k_{\text{obs}}$  vs [1] (Figure 5) a linear dependence with no intercept was observed confirming an irreversible reaction with the following rate law (eq. 1):

$$-\frac{d[\text{Ni}(\text{bipy})(\text{COD})]}{dt} = v = k_2 \cdot [5] \cdot [1] \quad (1)$$

From the slopes in Figure 5, second order rate constants  $k_2$  ( $k_{\text{obs}} = k_2 \cdot [1]$ ) were calculated and used for the Eyring plot presented in Figure 6. Activation parameters were determined leading to an activation enthalpy of  $\Delta H^\ddagger = 46.4 \pm 2 \text{ kJ} \cdot \text{mol}^{-1}$  and an activation entropy of  $\Delta S^\ddagger = -69 \pm 8 \text{ J} \cdot \text{mol}^{-1} \cdot \text{K}^{-1}$ . The negative activation entropy supports an associative or associative interchange mechanism with a highly ordered transition state.

Overall behavior, rate constants and activation parameters fit quite well with the data reported previously for the formation of other related nickel(0) complexes (Table 2). Therefore, the same mechanism can be postulated for the formation reaction (Scheme 2). For the transition state, a partial decoordination (**5 A**) of the leaving ligand COD followed by coordination of the attacking alkene in **5 B** is assumed, which emphasizes the associative element of the reaction mechanism. After the

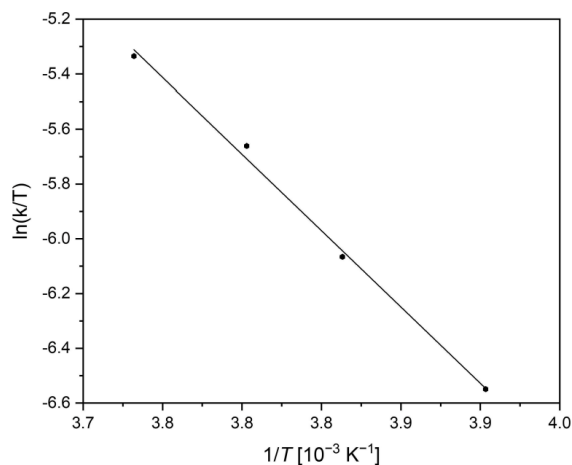
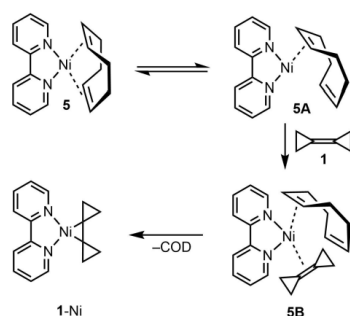


**Figure 6.** Eyring plot of the reaction to 1-Ni and linear fit (black line).

Table 2. Activation parameters for the formation of complexes 1-Ni, 3-Ni in comparison to selected literature examples.	bcp ( <b>1</b> )	dmbu ( <b>3</b> )	dimethyl 3-methyl-3- <i>tert</i> -butylcycloprop-1-ene-1,2-dicarboxylate ( <b>4</b> ) <sup>[38]</sup>	benzaldehyde <sup>[39]</sup>	isoprene <sup>[35]</sup>
$\Delta H^\ddagger$ [kJ·mol <sup>-1</sup> ]	46.4 ± 2.0	47.2 ± 3.0	28.0 ± 1.6	47.8 ± 0.4	35.0 ± 5.0
$\Delta S^\ddagger$ [J·K <sup>-1</sup> ·mol <sup>-1</sup> ]	-69 ± 8	-68 ± 10	-128 ± 5	-47 ± 1	-79 ± 16



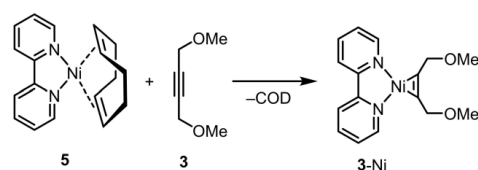
**Scheme 2.** Proposed mechanism for the formation of complex 1-Ni, as supported by the results of the kinetic measurements.

complete removal of the COD ligand, the final complex 1-Ni is formed in the last step.

Quite unexpectedly, in contrast to the kinetic study of **5** reacting with **1**, the investigation of the analogous reaction of the precursor complex **5** with **2** turned out to be more problematic. Although the reaction could be followed using the stopped-flow technique,<sup>[20]</sup> decomposition reactions hampered clean fitting of the data (time resolved UV-vis spectra are presented in Figure S1, Supporting Information). Again, a decrease of the band at 561 nm was observed for this reaction. This indicated the consumption of the precursor complex, whereas appearance of the bands at 410 and 805 nm showed the formation of the new complex 2-Ni. Isosbestic points were observed at 390 and 485 nm. The reactions had to be carried out at higher temperatures (10 to 25 °C vs. –5 to –20 °C), and observed reaction rates of **5** with **2** were somewhat slower in comparison with **1**. Despite applying pseudo first order conditions by using an excess of the ligand, no adequate fits of the absorbance vs. time plots were possible. Ignoring this and using  $k_{\text{obs}}$  values from poor fits to a single exponential function led to a plot of  $k_{\text{obs}}$  vs [2] with a linear behavior with an intercept (see Figure S2, Supporting Information). This indicates either a reversible formation of 2-Ni or a reaction type that would be independent from the concentration of **2**. As described in detail previously for related systems (e.g. isoprene in Table 2)<sup>[35]</sup> most likely it indicates a reversible reaction step. That no satisfying fits could be obtained is a consequence of decomposition reactions that seem to be more problematic here due to the higher temperatures that were necessary for the measurements. In contrast to our previous studies adding a tenfold excess of COD in this case did not prevent decomposition of **5** and thus did not solve the problem.

To find out whether this might be a general problem with coordinating alkynes in Ni(0) chemistry or a specific one for ligand **2**, another simple alkyne, 1,4-dimethoxy-2-butyne (**3**) was employed for the reaction with the precursor **5** (Scheme 3).

The time-resolved spectra of this reaction (see Figure S3, Supporting Information) with bands at 420 and 675 nm show the formation of the new complex [Ni(bipy)(dmbu)] (**3**-Ni) comparable to the other two complexes described above.<sup>[21]</sup>



**Scheme 3.** Reaction of **5** with 1,4-dimethoxy-2-butyne (**3**) to form **3**-Ni.

Unfortunately, no crystals of this complex could be obtained that were suitable for structural determination. The higher reaction temperatures applied are responsible for the blurred isosbestic points at 385 and 475 nm due to the slow decomposition of **5**. However, despite the observed decomposition and in contrast to the reaction with **2**, the decrease of the time trace at 561 nm could again be fitted to a single one-exponential function and the pseudo first-order rate constants  $k_{\text{obs}}$  could be determined from the plots with varying temperatures and ligand concentrations (see Figure S4, Supporting Information). The reaction is irreversible, as confirmed by the missing intercept of the linear fits, but in general very similar to the reaction with ligand **1**. This is again supported by the activation parameters that were calculated for the reaction with **3** as  $\Delta H^\ddagger = 47.2 \pm 3.0 \text{ kJ} \cdot \text{mol}^{-1}$  and  $\Delta S^\ddagger = -68 \pm 10 \text{ J} \cdot \text{mol}^{-1} \cdot \text{K}^{-1}$ , nearly identical to the data obtained for the reaction with **1**, despite the structural difference of the ligand scaffold.

These results indicate that the problems with the kinetic measurements for **2** as a ligand are not basic and caused by an alkyne moiety, but more likely are created specifically by the ligand **2** itself; probably due to steric encumbrance caused by the cyclopropyl groups, although the steric substituent constant of a cyclopropyl group, as defined by Beckhaus, is only slightly larger (1.33 versus 0.89) than that of an ethyl substituent.<sup>[37]</sup>

In summary, the kinetic studies for the reaction of **5** with several quite different ligands **L** showed that a general mechanism for the formation of the complexes [Ni(bipy)(L)] can be postulated (Scheme 2 with L = **1**).

**Oxygenation Reactions of 1-Cu and 2-Cu.** The ability of copper(I) complexes to stabilize a variety of “dioxygen adduct” intermediates has been investigated in great detail by us and others.<sup>[40]</sup> In this context, the lability of the bonding of **1** and **2** in these complexes prompted us to examine an oxygenation reaction of the latter. However, no intermediate complex was detectable in a benchtop experiment in which complexes 1-Cu and 2-Cu had been treated with dioxygen in acetone at –80 °C. Only a color change of the solution to a pale blue color could be observed caused by simple oxidation to the corresponding copper(II) complex. Furthermore, no oxidation of **1** and **2** was observed either. Workup of the solution of 2-Cu after oxidation led to the isolation of crystals of a copper(II) bipyridine complex, in which two Cu(II)(bipy) units are bridged by two hydroxide anions. The molecular structure of this complex could be determined, however no full refinement was performed on this compound because there are numerous examples of this complex type, e.g. [(bipy)Cu(OH)<sub>2</sub>Cu(bipy)](ClO<sub>4</sub>)<sub>2</sub><sup>[41]</sup> reported in the crystallographic database.

## Conclusion

Herein, we demonstrated that bicyclopropylidene (bcp) as well as dicyclopropylacetylene (dcpa), both valuable building blocks in organic syntheses, can be utilized as  $\eta^2$ -coordinating ligands for transition metal complexes. Copper(I) complexes of both ligands, [Cu(bipy)(bcp)]PF<sub>6</sub> and [Cu(bipy)(dcpa)]PF<sub>6</sub>, could be structurally characterized, however they turned out to be less interesting with regard to oxygenation chemistry (probably the consequence of 2,2'-bipyridine as a co-ligand). The molecular structures of the nickel(0) complexes, [Ni(bipy)(bcp)] and [Ni(bipy)(dcpa)], were determined as well and as expected turned out to be similar to the analogous copper complexes. The results of a detailed kinetic analysis on the formation of these two complexes are in line with previous studies of related complexes and underline a general mechanism for these reactions. In contrast to the copper complexes, [Ni(bipy)(bcp)] and [Ni(bipy)(dcpa)] might become useful in future catalytic applications. While extremely reactive, complexes of this type have been tested in the past for e.g. activation of otherwise quite unreactive carbon dioxide.<sup>[35,39]</sup> The problems with regard to handling these compounds can be overcome by starting with stable nickel(II) compounds and reducing these electrochemically thus performing electrocatalysis.<sup>[42]</sup>

## Experimental Section

**General Methods.** Commercially available reagents were used as obtained without further purification, unless otherwise stated. Anhydrous solvents were purchased from Acros Organics and further distilled three times over drying agents under Schlenk conditions. All experiments with air-sensitive compounds were carried out employing standard Schlenk techniques or in a glove box (MBraun, Garching, Germany; O<sub>2</sub> & H<sub>2</sub>O < 0.1 ppm) under an argon atmosphere. The ligands **1**<sup>[3]</sup> and **2**<sup>[17]</sup> were prepared as described previously. Complex **5** was chosen as a versatile precursor by us and others before,<sup>[26]</sup> therefore **5**<sup>[43]</sup> and [Cu(MeCN)<sub>4</sub>]PF<sub>6</sub><sup>[44]</sup> were synthesized according to the corresponding published procedures.

**Low Temperature Stopped-Flow Measurements.** Variable temperature stopped-flow measurements allowed the collection of time-resolved UV-vis spectra of the precursor complex reactions with the corresponding alkenes or alkynes as described previously.<sup>[35,39]</sup> The solutions were prepared in a glove box and transferred to the low-temperature stopped-flow instrument using glass syringes. The reactions were studied under pseudo-first-order conditions with an excess of ligand solution. Temperatures were varied from -20 to 35 °C. Time-resolved UV-vis spectra of these reactions were recorded with a home-built stopped-flow unit or with a modified Hi-Tech SF-3 L low-temperature stopped-flow unit (Salisbury, UK) equipped with a J&M TIDAS 16-500 photodiode array spectrophotometer (J&M, Aalen, Germany).<sup>[45]</sup> Data fitting was performed using the integrated Kinetic Studio 4.0 software package (TgK Scientific, Bradford-on-Avon, UK) and Origin 2018 (OriginLab Corporation, Northampton, USA).

**Single-Crystal X-ray Structure Determinations.** The diffraction experiments were carried out under inert conditions at 193 K on a Siemens SMART CCD 1000 diffractometer and a STOE IPDS diffractometer using graphite monochromated Mo- K $\alpha$  radiation ( $\lambda = 0.71073$  Å). The structures were solved by direct methods using

SHELXS and refined against F<sup>2</sup> on all data by full-matrix least squares with SHELXL.<sup>[46]</sup> Details of the crystal and refinement data are described in the Supporting Information.

**8,11-Diaza-8:9,10:11-dibenzo-7-nickeltrispiro[2.0.2<sup>4</sup>.0.4<sup>7</sup>.0<sup>3</sup>] undeca-8,10-diene [Ni(bipy)(bcp)] (1-Ni):** To a stirred suspension of [Ni(bipy)(COD)] (200 mg, 619  $\mu$ mol) in Et<sub>2</sub>O (10 mL) was added **1** (210 mg, 246  $\mu$ L, 2.62 mmol) and the reaction mixture was stirred until the solution turned dark green. The green solid was filtered off, washed with Et<sub>2</sub>O two times and dried in vacuo. Yield: 94 mg (51%). Suitable crystals for X-ray characterization were obtained by vapor diffusion of *n*-pentane into a solution in THF. <sup>1</sup>H NMR (400 MHz, acetone-d<sub>6</sub>):  $\delta = 8.91$  (d, 2 H), 8.15 (m, 4 H), 7.55 (t, 2 H), 0.67 (s, 4 H), 0.22 (s, 4 H) ppm.

**8,11-Diaza-8:9,10:11-dibenzo-7-nickeltrispiro[2.0.2<sup>4</sup>.0.4<sup>7</sup>.0<sup>3</sup>] undeca-8,10-diene Hexafluorophosphate [Cu(bipy)(bcp)]PF<sub>6</sub> (1-Cu):** [Cu(MeCN)<sub>4</sub>]PF<sub>6</sub> (37.2 mg, 0.10 mmol) and 2,2'-bipyridine (15.6 mg, 0.10 mmol) were dissolved in acetone (3 mL). After addition of **1** (16.0 mg, 18.7  $\mu$ L, 0.2 mmol), the reaction mixture was stirred for an additional 10 min until the color of the solution turned to pale yellow. Vapor diffusion of diethyl ether into the solution yielded single crystals of the complex suitable for X-ray characterization. <sup>1</sup>H NMR (400 MHz, acetone-d<sub>6</sub>):  $\delta = 8.96$  (d, 2 H), 8.70 (d, 2 H), 8.36 (t, 2 H), 7.87 (t, 2 H), 1.59 (br s, 8 H) ppm. <sup>13</sup>C NMR (100 MHz, acetone-d<sub>6</sub>):  $\delta = 153.9, 151.1, 143.1, 129.3, 124.3, 9.1$  ppm.

**[Ni(bipy)(dcpa)] (2-Ni):** To a stirred solution of [Ni(bipy)(COD)] (3.2 mg, 9.9  $\mu$ mol) in THF (2 mL), a solution of alkyne **2** (106 mg, 1.0 mmol) in THF (2 mL) was added dropwise at -20 °C. The resulting solution was stirred for two hours and filtered through a pad of zeolite. Diffusion of *n*-pentane into the solution at -5 °C afforded the single crystals suitable for X-ray structure determination.

**[Cu(bipy)(dcpa)]PF<sub>6</sub> (2-Cu):** [Cu(MeCN)<sub>4</sub>]PF<sub>6</sub> (37.2 mg, 0.1 mmol) and 2,2'-bipyridine (15.6 mg, 0.10 mmol) were dissolved in acetone (3 mL). Alkyne **2** (38.8 mg, 365  $\mu$ mol) was added and after 10 minutes stirring the solution turned pale yellow. Crystals of the yellow-orange solid suitable for X-ray characterization were obtained by slow diffusion of diethyl ether into the solution at -5 °C during several days.

**Attempted Isolation of Crystalline [Ni(bipy)(dmbu)] (3-Ni):** To a stirred solution of [Ni(bipy)(COD)] (25.8 mg, 79.8  $\mu$ mol) in THF was added ligand **3** (2 mL) (116 mg, 1.02 mmol). The resulting dark red solution was stirred for one hour. Diffusion of *n*-pentane into the solution at -20 °C did not result in crystals suitable for X-ray structure determination so far.

Deposition Numbers 2052272 (1-Ni), 2052271 (2-Ni), 2052273 (1-Cu), and 2052274 (2-Cu) contain the supplementary crystallographic data for this paper. These data are provided free of charge by the joint Cambridge Crystallographic Data Centre and Fachinformationszentrum Karlsruhe Access Structures service [www.ccdc.cam.ac.uk/structures](http://www.ccdc.cam.ac.uk/structures).

## Acknowledgements

*We sincerely thank Lars Römmling for his previously performed preliminary experiments during his diploma thesis on nickel complexes with bcp. Open access funding enabled and organized by Projekt DEAL.*

## Conflict of Interest

The authors declare no conflict of interest.

**Keywords:** Alkene complexes · Copper(I) complexes · Crystallography · Kinetics · Nickel(0) complexes

- [1] L. Zhao, A. de Meijere, *Adv. Synth. Catal.* **2006**, *348*, 2484–2492.
- [2] A. de Meijere, S. I. Kozhushkov, T. Spaeth, N. S. Zefirov, *J. Org. Chem.* **1993**, *58*, 502–505.
- [3] A. de Meijere, S. I. Kozhushkov, T. Späth in *Organic Syntheses*, John Wiley & Sons, Inc, Hoboken, NJ, USA, **2003**, pp. 142–151.
- [4] A. de Meijere, S. I. Kozhushkov, A. F. Khlebnikov in *Topics in Current Chemistry* (Eds.: A. de Meijere, K. N. Houk, H. Kessler, J.-M. Lehn, S. V. Ley, S. L. Schreiber, J. Thiem, B. M. Trost, F. Vögtle, H. Yamamoto), Springer, Berlin, Heidelberg, **2000**, pp. 89–147.
- [5] a) A. de Meijere, S. I. Kozhushkov, *Eur. J. Org. Chem.* **2000**, 3809–3822; b) A. de Meijere, S. I. Kozhushkov, T. Späth, M. von Seebach, S. Löhr, H. Nüske, T. Pohlmann, M. Es-Sayed, S. Bräse, *Pure Appl. Chem.* **2000**, *72*, 1745–1756; c) A. de Meijere, S. I. Kozhushkov, H. Schill, *Chem. Rev.* **2006**, *106*, 4926–4996; d) A. de Meijere, *Org. Synth.* **2018**, *95*, 289–309; e) A. de Meijere, K. N. Houk, H. Kessler, J.-M. Lehn, S. V. Ley, S. L. Schreiber, J. Thiem, B. M. Trost, F. Vögtle, H. Yamamoto (Eds.) *Topics in Current Chemistry*, Springer, Berlin, Heidelberg, **2000**.
- [6] A. de Meijere, S. I. Kozhushkov, *Chem. Rev.* **2000**, *100*, 93–142.
- [7] I. Nakamura, Y. Yamamoto, *Adv. Synth. Catal.* **2002**, *344*, 111–129.
- [8] a) P. Binger, P. Wedemmann, S. I. Kozhushkov, A. de Meijere, *Eur. J. Org. Chem.* **1998**, 113–119; b) M. Schelper, O. Buisine, S. Kozhushkov, C. Aubert, A. de Meijere, M. Malacria, *Eur. J. Org. Chem.* **2005**, 3000–3007; c) A. Demircan, *Molecules* **2014**, *19*, 6058–6069.
- [9] J. Foerstner, H. Butenschön, S. Kozhushkov, P. Binger, A. de Meijere, P. Wedemmann, M. Noltemeyer, *Chem. Commun.* **1998**, 239–240.
- [10] S. I. Kozhushkov, J. Foerstner, A. Kakoschke, D. Stellfeldt, L. Yong, R. Wartchow, A. de Meijere, H. Butenschön, *Chem. Eur. J.* **2006**, *12*, 5642–5647.
- [11] P. Hofmann, A. de Meijere, F. Romminger, S. I. Kozhushkov, H. Schill, C. Reitmeyer, *unpublished results*.
- [12] S. A. Hoyte, J. L. Spencer, *Organometallics* **2011**, *30*, 5415–5423.
- [13] H. Weiss, F. Hampel, W. Donaubaue, M. A. Grundl, J. W. Bats, A. S. K. Hashmi, S. Schindler, *Organometallics* **2001**, *20*, 1713–1715.
- [14] a) G. Köbrich, D. Merkel, *Angew. Chem. Int. Ed. Engl.* **1970**, *9*, 243–244; *Angew. Chem.* **1970**, *82*, 255–255; b) G. Köbrich, D. Merkel, K.-W. Thiem, *Chem. Ber.* **1972**, *105*, 1683–1693.
- [15] H.-C. Militzer, S. Schömenauer, C. Otte, C. Puls, J. Hain, S. Bräse, A. de Meijere, *Synthesis* **1993**, *1993*, 998–1012.
- [16] S. C. Suri, J. C. Marcischak, *Org. Prep. Proced. Int.* **2013**, *45*, 154–161.
- [17] L. T. Scott, M. J. Cooney, C. Otte, C. Puls, T. Haumann, R. Boese, A. B. Smith, P. J. Carroll, A. de Meijere, *J. Am. Chem. Soc.* **1994**, *116*, 10275–10283.
- [18] a) A. de Meijere, S. Redlich, S. I. Kozhushkov, D. S. Yufit, J. Magull, D. Vidović, H. Schill, H. Menzel, *Eur. J. Org. Chem.* **2012**, 6953–6958; b) I. Emme, T. Labahn, A. de Meijere, *Eur. J. Org. Chem.* **2006**, 399–404.
- [19] a) Z. Mo, J. Xiao, Y. Gao, L. Deng, *J. Am. Chem. Soc.* **2014**, *136*, 17414–17417; b) L. Yong, K. Kirleis, H. Butenschön, *Adv. Synth. Catal.* **2006**, *348*, 833–836.
- [20] A. Henß, *Dissertation*, Justus-Liebig-Universität, Gießen, **2008**.
- [21] L. Valentin, *Dissertation*, Justus-Liebig-Universität, Gießen, **2014**.
- [22] a) M. von Seebach, S. I. Kozhushkov, R. Boese, J. Benet-Buchholz, D. S. Yufit, J. A. K. Howard, A. de Meijere, *Angew. Chem.* **2000**, *112*, 2617–2620; *Angew. Chem. Int. Ed.* **2000**, *39*, 2495–2498; b) A. de Meijere, M. von Seebach, S. Zöllner, S. I. Kozhushkov, V. N. Belov, R. Boese, T. Haumann, J. Benet-Buchholz, D. S. Yufit, J. A. K. Howard, *Chem. Eur. J.* **2001**, *7*, 4021–4034.
- [23] K. Hagen, L. Hedberg, K. Hedberg, *J. Phys. Chem.* **1982**, *86*, 117–121.
- [24] B. R. Özer, I. Heo, J. C. Lee, C. Schröter, T. Schultz, *Phys. Chem. Chem. Phys.* **2020**, *22*, 8933–8939.
- [25] N. Yasuda, H. Uekusa, Y. Ohashi, *Acta Crystallogr. Sect. E* **2001**, *57*, 1189–1190.
- [26] A. E. King, S. C. E. Stieber, N. J. Henson, S. A. Kozimor, B. L. Scott, N. C. Smythe, A. D. Sutton, J. C. Gordon, *Eur. J. Inorg. Chem.* **2016**, *2016*, 1635–1640.
- [27] Y. Zhao, Z. Wang, X. Jing, Q. Dong, S. Gong, Q.-S. Li, J. Zhang, B. Wu, X.-J. Yang, *Dalton Trans.* **2015**, *44*, 16228–16232.
- [28] W. Mayer, G. Wilke, R. Benn, R. Goddard, C. Krüger, *Monatsh. Chem.* **1985**, *116*, 879–888.
- [29] M. Maekawa, M. Munakata, T. Kuroda-Sowa, K. Hachiya, *Inorg. Chim. Acta* **1995**, *232*, 231–234, and refs. [17–19] cited therein.
- [30] M. Dakkouri, V. Typke, R. Bitschenauer, *J. Mol. Struct.* **1995**, *355*, 239–263.
- [31] J. J. Eisch, X. Ma, K. I. Han, J. N. Gitua, C. Krüger, *Eur. J. Inorg. Chem.* **2001**, 77–88.
- [32] R. Thomas, S. Lakshmi, S. K. Pati, G. U. Kulkarni, *J. Phys. Chem. B* **2006**, *110*, 24674–24677.
- [33] J. S. Thompson, J. F. Whitney, *Inorg. Chem.* **1984**, *23*, 2813–2819.
- [34] F. H. Allen, *Acta Crystallogr. Sect. B* **1980**, *36*, 81–96.
- [35] C. Geyer, S. Schindler, *Organometallics* **1998**, *17*, 4400–4405.
- [36] a) T. Yamamoto, A. Yamamoto, S. Ikeda, *J. Am. Chem. Soc.* **1971**, *93*, 3350–3359; b) T. Yamamoto, A. Yamamoto, S. Ikeda, *J. Am. Chem. Soc.* **1971**, *93*, 3360–3364.
- [37] H.-D. Beckhaus, *Angew. Chem. Int. Ed. Engl.* **1978**, *17*, 593–594; *Angew. Chem.* **1978**, *90*, 633–635.
- [38] Helmut Weiss, *Dissertation*, Friedrich-Alexander-Universität, Erlangen-Nürnberg, **2001**.
- [39] C. Geyer, E. Dinjus, S. Schindler, *Organometallics* **1998**, *17*, 98–103.
- [40] J. J. Liu, D. E. Diaz, D. A. Quist, K. D. Karlin, *Isr. J. Chem.* **2016**, *56*, 9–10.
- [41] M. Toofan, A. Boushehri, M.-U.-H. Mazhar-UI-Haque, *J. Chem. Soc. Dalton Trans.* **1976**, 217–219.
- [42] K. I. Alexopoulou, M. Leibold, O. Walter, T. A. Zevaco, S. Schindler, *Eur. J. Inorg. Chem.* **2017**, 4722–4732.
- [43] a) B. Heyn, B. Hipler, G. Kreisel, H. Schreer, D. Walther, *Anorganische Synthesechemie: Ein integriertes Praktikum*, Springer Verlag, Berlin, Heidelberg, New York, Tokyo, **1990**; b) G. W. Parshall, *Inorganic Syntheses*, McGraw-Hill Book Company, New York, **1974**; c) P. Binger, M. J. Doyle, J. McMeeking, C. Krüger, Y.-H. Tsay, *J. Organomet. Chem.* **1977**, *135*, 405–414.
- [44] D. F. Shriver, *Inorganic Syntheses*, John Wiley & Sons, Inc, New York, **1979**.
- [45] M. Weitzer, M. Schatz, F. Hampel, F. W. Heinemann, S. Schindler, *J. Chem. Soc. Dalton Trans.* **2002**, 686–694.
- [46] a) G. M. Sheldrick, *Acta Crystallogr. Sect. A* **2015**, *71*, 3–8; b) G. M. Sheldrick, *Acta Crystallogr. Sect. A* **2008**, *64*, 112–122.

Manuscript received: January 15, 2021  
Revised manuscript received: February 10, 2021  
Accepted manuscript online: February 14, 2021

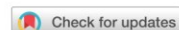
---

#### 4. Kinetic investigations of the formation of iron(IV) oxido complexes

This work has been published in  
*Journal of Coordination Chemistry*

Florian J. Ritz, Markus Lerch, Jonathan Becker, Siegfried Schindler

*J. Coord. Chem.*, **2022**, 75, 894-907.  
doi.org/10.1080/00958972.2022.2095268



## Kinetic investigations of the formation of iron(IV) oxido complexes

Florian J. Ritz, Markus Lerch, Jonathan Becker and Siegfried Schindler 

Institut für Anorganische und Analytische Chemie, Justus-Liebig-Universität Gießen, Gießen, Germany

### ABSTRACT

Oxido iron(IV) complexes are key intermediates in oxygenation reactions in biological systems. They can form during oxidation experiments with various oxidants such as oxygen, hydrogen peroxide, organoiodine compounds, or ozone. However, kinetic studies for these reactions are rare because the intermediates are usually labile. Here the results of a detailed investigation on the oxidation of iron(II) complexes with macrocyclic (e.g. TMC = tetramethylcyclam = 1,4,8,11-tetramethyl-1,4,8,11-tetraaza-cyclotetradecane) ligands are reported that provide a better understanding of the mechanisms of these reactions. For formation of the quite stable oxido iron complex with an amide derivative of TMC, activation parameters with  $\Delta H^\ddagger = 28 \pm 4 \text{ kJ}\cdot\text{mol}^{-1}$  and  $\Delta S^\ddagger = -144 \pm 15 \text{ J}\cdot\text{mol}^{-1}\cdot\text{K}^{-1}$  could be obtained that allowed postulation of an associative mechanism.

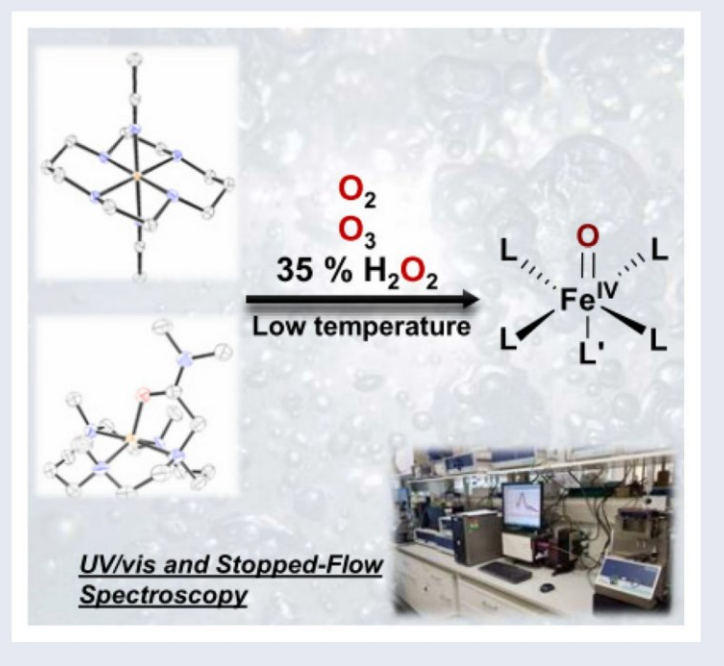
### ARTICLE HISTORY

Received 29 March 2022

Accepted 14 June 2022

### KEYWORDS

Iron; chromium; dioxygen activation; oxido complexes; kinetics



**CONTACT** Siegfried Schindler [Siegfried.Schindler@ac.jlug.de](mailto:Siegfried.Schindler@ac.jlug.de)  Institut für Anorganische und Analytische Chemie, Justus-Liebig-Universität Gießen, Heinrich-Buff-Ring 17, Gießen, 35392, Germany

 Supplemental data for this article is available online at <https://doi.org/10.1080/00958972.2022.2095268>.

© 2022 Informa UK Limited, trading as Taylor & Francis Group

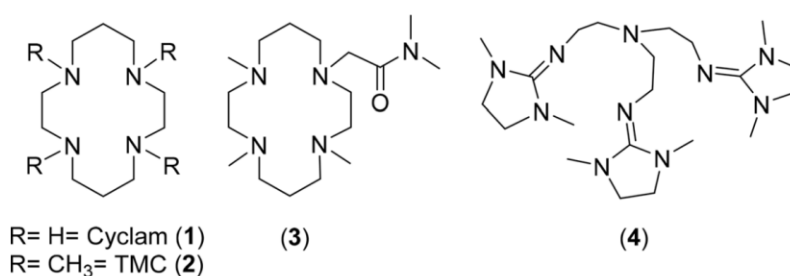
## 1. Introduction

Non-heme iron enzymes play a key role in selective conversions of organic substrates and are capable of catalyzing a variety of reactions, including hydroxylation of aromatic and aliphatic hydrocarbons, desaturation, epoxidation, *cis*-dihydroxylation, halogenation etc. [1]. There has been increased interest in bioinorganic research, as evidenced by the growing number of reports of model complexes by oxygen activation in cytochrome P450 or similar enzymes [2]. The extensively studied dioxygen activation of these complexes occurs in many cases through, for example, superoxido, peroxido or hydroperoxido species as intermediates [3]. In biomimetic chemistry, high-valent oxido-Fe(IV) complexes (former nomenclature oxo-Fe) have been of interest for two decades due to their importance in enzymatic catalytic cycles [1, 4]. Since the first report of a full characterization of a nonheme-Fe(IV)-oxido complex with the macrocyclic ligand tetramethylcyclam (TMC = 1,4,8,11-tetramethyl-1,4,8,11-tetraaza-cyclotetradecane, **2**, Scheme 1) by Rohde *et al.* in 2003 [5], a large number of new high valent Fe(IV)-species have been reported [6]. In a typical synthetic procedure the precursor complexes are treated with an excess of oxidant, mainly organoiodine compounds or aqueous solutions of hydrogen peroxide, at low temperatures to stabilize the often short-living and labile species [7]. In contrast, we have started to use ozone as an oxidant [8], which has rarely been used in the oxygen activation of coordination compounds [9]. Advantages of ozone are that it is introduced as a highly reactive gas into the solutions without solubility problems (iodosylbenzene) or introduction of water (aqueous hydrogen peroxide). Furthermore, it enables reactions at low temperatures that in many cases would not take place at all [8]. In enzymatic transformations, the O<sub>2</sub> molecule has to be activated first (to overcome the spin forbidden reaction of the triplet ground state) to a superoxido complex that in further consecutive reactions leads to the oxido species. Therefore, only a few examples of a direct conversion with O<sub>2</sub> to the Fe(IV)-oxido complex analogous to the biological models are known [1]. In this context, Ray and co-workers recently reported excellent work on formation of the Fe(IV)-oxido complex with cyclam (1,4,8,11-tetraaza-cyclotetradecane, **1**, Scheme 1) in a direct reaction with oxygen [10].

Modification of the TMC ligand by appending a *N,N*-dimethylacetamide donor to the macrocycle (1,4,8-Me<sub>3</sub>cyclam-11-CH<sub>2</sub>C(O)NMe<sub>2</sub>, **3**, Scheme 1) led to formation of a quite stable Fe(IV) oxido complex by reacting the corresponding iron(II) complex with iodosylbenzene in acetonitrile [11].

Besides N-tetradentate macrocycles tripodal ligand other systems have been applied; here especially the guanidine substituted tris-{2-aminoethyl}amine (tren) framework turned out to be suitable to support formation of an Fe(IV) oxido complex [12, 13]. In 2009, England *et al.* reported the synthesis and spectroscopic characterization of a high spin iron(IV) oxido complex with TMG<sub>3</sub>tren (1,1,1-tris{2-[N<sup>2</sup>-(1,1,3,3-tetramethylguanidino)]ethyl}amine) as a ligand [14]. Preventing a methyl-group oxidative self-decay by deuteration of the methyl groups, they were able to obtain a high quality molecular structure in 2010 of this complex [15]. The tripodal ligand DMEG<sub>3</sub>tren (**4**) in Scheme 1 is a sterically more restrictive derivative of TMG<sub>3</sub>tren [16].

The usually observed thermal instability and high reactivity of the oxido iron(IV) complexes towards organic substrates had to be overcome to investigate their



**Scheme 1.** Overview of ligands used in this work.

structural and spectroscopic properties. This is one of the main reasons why few detailed kinetic studies of these complexes have been reported so far. However, reaction parameters are of particular relevance for an understanding of the basic mechanisms and future technical applications of oxygenation reactions. Therefore, herein, we present a more detailed kinetic investigation of reactions leading to iron(IV) oxido complexes under different conditions.

## 2. Results and discussion

### 2.1. Direct oxygenation of *trans*-[Fe(1)(MeCN)<sub>2</sub>](OTf)<sub>2</sub> with O<sub>2</sub>

As described above, Ray and co-workers recently succeeded in obtaining the Fe(IV) oxido complex with cyclam (1) as a ligand through a direct reaction of the corresponding iron(II) triflate complex with dioxygen [10]. The interesting observation is that *trans*-[Fe(1)(MeCN)(O)](OTf)<sub>2</sub> directly forms without electrons and protons provided additionally (as for e.g. Cyt. P450) [17] or by an oxygen atom transfer (OAT) reaction [10]. Therefore, as pointed out by Ray and co-workers, *trans*-[Fe(1)(MeCN)(O<sub>2</sub>)](OTf)<sub>2</sub> might represent the first product of the reaction of dioxygen with the diiron active site in methane monooxygenase (MMO) [10].

We were able to reproduce the findings of the Ray group and observed the fast reaction to the assigned Fe(III) superoxido complex, *trans*-[Fe(1)(MeCN)(O<sub>2</sub>)](OTf)<sub>2</sub> (with  $\lambda_{\text{max}}$  at 330 nm, see Figure 1). This is immediately followed by formation of the Fe(IV) oxido complex, characterized by absorbance maxima at 584 and 690 nm with nearly equal intensity. Detailed spectroscopic data for both complexes have been reported and an overall mechanism for the reaction proposed [10]. However, we find reason to disagree with the previous worker's hypothesis of a second order dependence of the iron complex and certain aspects of the resulting complicated explanation of the mechanism.

Due to our general interest in the formation of superoxido complexes with transition metals [13, 18], we performed stopped-flow measurements in acetone at  $-60.1$  °C for formation of *trans*-[Fe(1)(MeCN)(O<sub>2</sub>)](OTf)<sub>2</sub> under the same conditions as reported by Ray and co-workers, and time resolved spectra are presented in Figure 1. The absorbance time traces at all wavelengths could be fitted perfectly to the sum of two exponential functions. An example of a fit at 333 nm is shown as an inset in Figure 1 (data points and fit). These kinds of fits are typically seen in consecutive reactions [19]

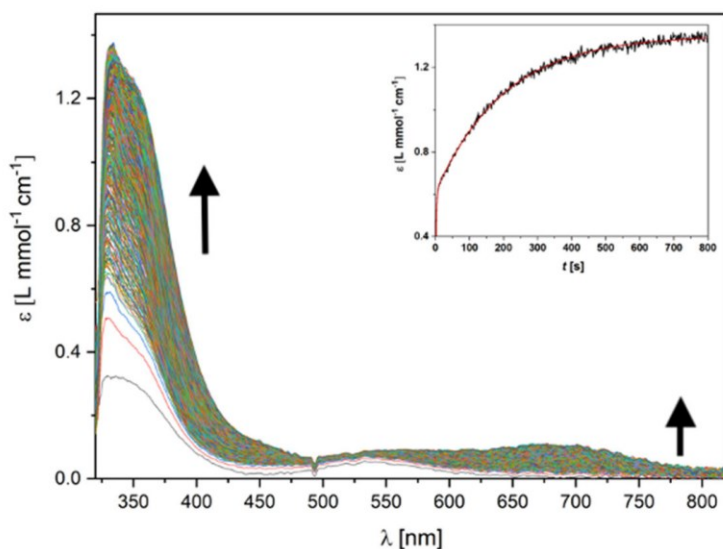
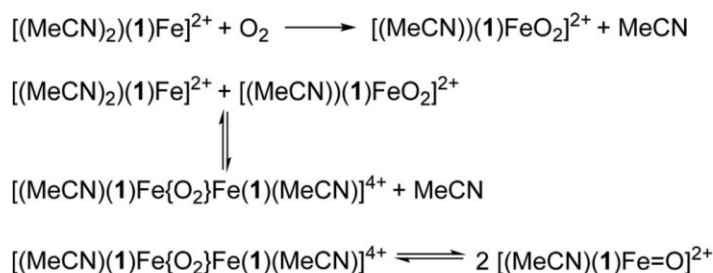


**Figure 1.** Time resolved UV-vis spectra of the reaction of  $[\text{Fe}(\mathbf{1})(\text{MeCN})_2](\text{OTf})_2$  with  $\text{O}_2$  in acetone, 500 scans,  $t = 500$  s,  $\Delta t = 1$  s,  $-60.1$  °C,  $[\text{complex}] = 0.75$  mmol/L,  $[\text{O}_2] = 5.92$  mmol/L; Inset: extinction coefficient ( $\epsilon$ ) vs. time trace at 333 nm with a fit of the sum of two exponential functions (red).



**Scheme 2.** Proposed mechanism for the formation of *trans*- $[\text{Fe}(\mathbf{1})(\text{MeCN})(\text{O})](\text{OTf})_2$ .

which is in accord with the observation that the iron oxido complex is formed after formation of the superoxido complex. Comparable observations were also possible at higher temperatures, for example at  $-20$  °C, where Ray and co-workers had performed their measurements. To further support our mechanistic description, we additionally obtained plots of the observed rate constants  $k_{\text{obs}}(\text{faster})$  and  $k_{\text{obs}}(\text{slower})$  vs. dioxygen concentration (Figures S1a and S1b). The larger rate constant showed a linear dependence on  $[\text{O}_2]$  with no intercept ( $k_{\text{obs}} = k \cdot [\text{O}_2]$ ), while the smaller rate constant is independent of  $[\text{O}_2]$  ( $k_{\text{obs}} = k$ ). The overall findings thus are in accord with the mechanism shown in Scheme 2.

In a first step the superoxido complex *trans*- $[\text{Fe}(\mathbf{1})(\text{MeCN})(\text{O}_2)](\text{OTf})_2$  is formed in an irreversible reaction (no intercept in plot of  $k_{\text{obs}}$  vs.  $[\text{O}_2]$ ) that further reacts with starting material *trans*- $[\text{Fe}(\mathbf{1})(\text{MeCN})_2](\text{OTf})_2$  to an intermediate in the rate determining step. This intermediate cannot be spectroscopically detected (steady state conditions) because it immediately reacts further (breaks apart) to the final product, the oxido complex *trans*- $[\text{Fe}(\mathbf{1})(\text{MeCN})(\text{O})](\text{OTf})_2$  ( $k_{\text{obs}}$  independent on  $[\text{O}_2]$ ). The intermediate

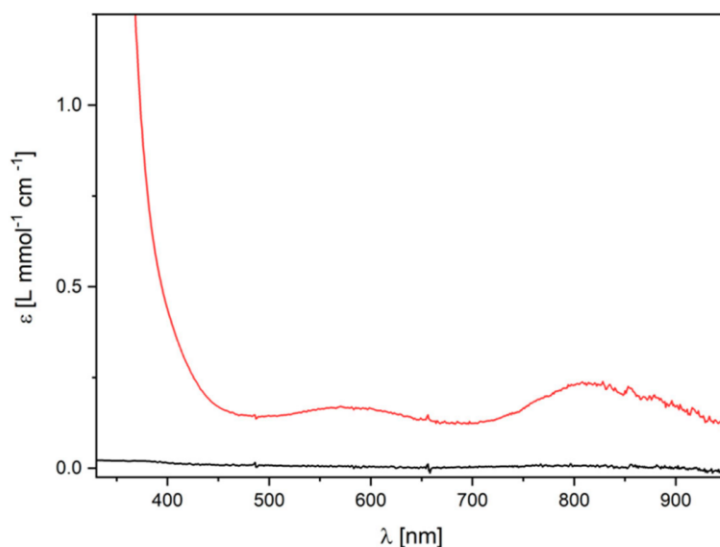


**Figure 2.** Reaction of  $[\text{Fe}(\mathbf{2})(\text{OTf})](\text{OTf})$  (black line) in dcm at  $-80^\circ\text{C}$  with ozone: Formation of the oxido iron(IV) species (red line),  $[\text{complex}] = 2 \text{ mmol/L}$ .

most likely is either a dinuclear peroxido iron(III) or *bis- $\mu$ -oxido* iron(IV) complex as suggested by Ray and co-workers [10].

We previously reported a full kinetic analysis of a comparable copper complex system, where a dinuclear *side-on* peroxido copper(II) complex is formed from the reaction of two mononuclear copper(I) complexes with dioxygen according to the following equations (charges are omitted,  $L = \text{tris}[2-(1,4\text{-diisopropylimidazolyl})]\text{phosphine}$ ) [20],



## 2.2. Reactions of ozone and hydrogen peroxide with $[\text{Fe}(\mathbf{2})(\text{OTf})](\text{OTf})$

As discussed above, formation of the oxido complex *trans*- $[\text{Fe}(\mathbf{1})(\text{MeCN})(\text{O}_2)](\text{OTf})_2$  from an iron(II) compound and dioxygen as the sole oxidant is exceptional. Usually, stronger oxidants such as hydrogen peroxide or iodoso benzene (or derivatives) need to be applied [21]. With both oxidants, the oxido iron(IV) complex  $[\text{Fe}=\text{O}(\mathbf{2})](\text{OTf})_2$  could be obtained [5]. In TMC (**2**), in contrast to cyclam (**1**), all hydrogen atoms are substituted by methyl groups, often an advantage with regard to stabilities of high valent "oxygen adduct" complexes [22]. Previously we could synthetically obtain  $[\text{Fe}=\text{O}(\mathbf{2})](\text{OTf})_2$  in high yields by reacting solvent free  $[\text{Fe}(\mathbf{2})(\text{OTf})](\text{OTf})$  with ozone in dcm (a very clean reaction without side products) [8]. Spectroscopically we could observe the formation of  $[\text{Fe}=\text{O}(\mathbf{2})](\text{OTf})_2$  by low-temperature UV-vis measurements. An UV-vis spectrum of this complex with absorbance maxima at 570 and 820 nm is presented in Figure 2. It was obtained by treating  $[\text{Fe}(\mathbf{2})(\text{OTf})](\text{OTf})$  with ozone for 30 s at  $-80^\circ\text{C}$  in dcm. It is important to note that  $[\text{Fe}(\mathbf{2})(\text{OTf})](\text{OTf})$  does not react with dioxygen under these conditions. No

intermediate was detected in that reaction, however, it is most likely that an ozonido iron(III) complex will form that then reacts further to  $[\text{Fe}=\text{O}(\mathbf{2})](\text{OTf})_2$ . No fully characterized ozonido complexes of transition metals have been reported yet. So far, only ozonides of alkali metals and  $\text{NMe}_4\text{O}_3$  have been described in detail [23, 24]. Therefore, we tried to observe the hypothesized short-lived ozonido complex  $[\text{Fe}(\mathbf{2})(\text{O}_3)](\text{OTf})_2$  by using low temperature stopped-flow techniques. However, while ozone was perfectly suited for our synthetic applications it did not work at all for the kinetic studies. The concentration of ozone in the reactant syringe was too low to observe the reaction spectroscopically. Ozone obtained from our generator produces a mixture of 6–14% ozone and 86–94% dioxygen (depending on the gas pressure, time and current settings; max. concentration). This mixture is then bubbled through dcm in our reactant syringe and thus high enough concentrations of ozone cannot be achieved.

Furthermore, we performed a kinetic investigation of the reaction of  $[\text{Fe}(\mathbf{2})(\text{OTf})](\text{OTf})$  with hydrogen peroxide in acetonitrile. However, while we do see the reaction taking place, side reactions were observed and no clean data fitting could be achieved. Kinetic studies with iodosylbenzene were not performed due to solubility problems under stopped-flow conditions.

### 2.3. Reactions of ozone and hydrogen peroxide $[\text{Fe}(\mathbf{3})](\text{OTf})_2$

With a derivative of the TMC ligand, 1,4,8-Me<sub>3</sub>cyclam-11-CH<sub>2</sub>C(O)NMe<sub>2</sub> (**3**, Scheme 1), an ultra-stable Fe(IV) oxido complex had been reported [11]. We prepared **3** according to the literature through a bridged tricyclo derivative of cyclam [25] which then was modified by introducing an amide group [26]. The corresponding iron(II) complex  $[\text{Fe}(\mathbf{3})](\text{OTf})_2$  was obtained and characterized as described by England et al. [11]. We also obtained crystals suitable for structural characterization, similar to the reported data (the molecular structure and crystallographic data are reported in the Supporting Information, Figure S4). Interestingly due to an excess of iodide ions in one batch of the ligand synthesis, the iron(II) complex  $[\text{Fe}(\mathbf{3})](\text{FeI}_4)$  was obtained and structurally characterized (the molecular structure and crystallographic data are reported in the Supporting Information, Figure S3).

As described above for  $[\text{Fe}(\mathbf{2})](\text{OTf})_2$ , while ozone can be used for synthetic applications, its concentration unfortunately is not high enough for kinetic studies using stopped-flow measurements. However, in contrast to  $[\text{Fe}(\mathbf{2})](\text{OTf})_2$  it was possible to investigate the reaction of  $[\text{Fe}(\mathbf{3})](\text{OTf})_2$  with hydrogen peroxide in more detail. Time resolved UV-vis spectra are presented in Figure 3. The reaction, performed under pseudo-first order conditions (large excess of hydrogen peroxide) was quite slow and the absorbance vs. time traces could be fitted quite well to a single exponential function (see inset in Figure 3), thus leading to a first order rate law with:

$$d[\text{oxido complex}]/dt = k_{\text{obs}} \cdot c[[\text{Fe}(\mathbf{3})](\text{OTf})_2]$$

Measurements with different concentrations of hydrogen peroxide and temperatures from  $-40.0$  to  $-10.0$  °C allowed a plot of  $k_{\text{obs}}$  versus  $[\text{H}_2\text{O}_2]$  (presented in Figure 4). The linear fits without an intercept demonstrated that the reaction is irreversible and shows first order dependence on the hydrogen peroxide as well (with  $k_{\text{obs}} =$

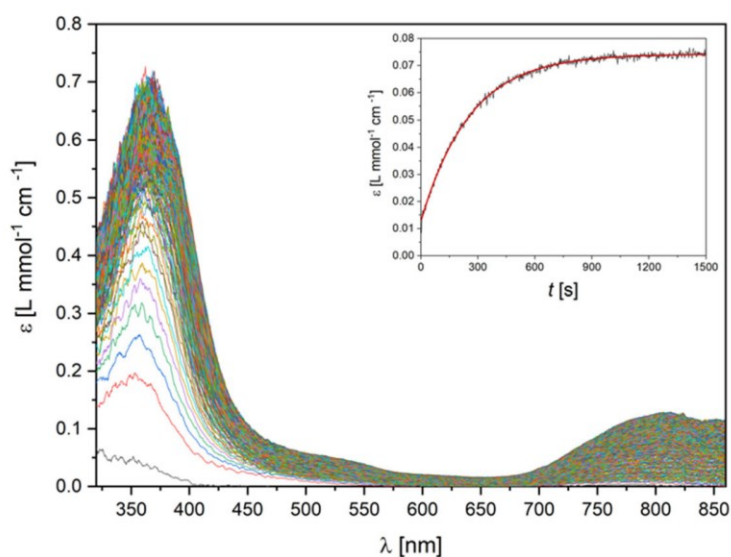


**Figure 3.** Time resolved UV-vis spectra of the reaction of  $[\text{Fe}(\mathbf{3})](\text{OTf})_2$  with 20 eq. of  $\text{H}_2\text{O}_2$  (35%) in MeCN,  $-40.0\text{ }^\circ\text{C}$ , 500 spectra,  $t = 1500\text{ s}$ ,  $\Delta t = 3\text{ s}$ ;  $[\text{complex}] = 1.5\text{ mmol/L}$ ,  $[\text{H}_2\text{O}_2] = 30\text{ mmol/L}$ ; Inset: extinction coefficient ( $\epsilon$ ) vs. time trace at 820 nm with a single exponential fit (red).

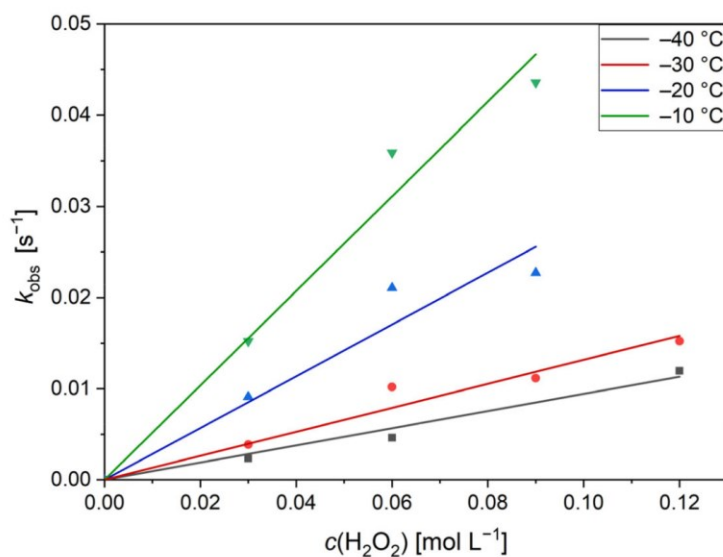
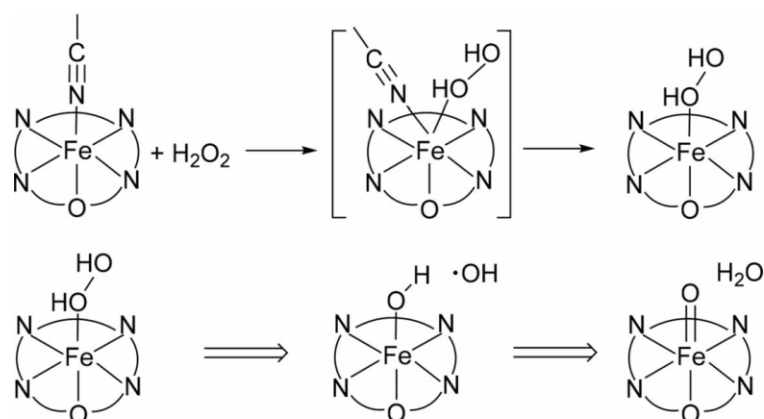


**Figure 4.** Plot of  $k_{\text{obs}}$  vs.  $c(\text{H}_2\text{O}_2)$  at four different temperatures from  $-40$  (black) to  $-10$   $^\circ\text{C}$  (green) with linear fits for the reaction of  $[\text{Fe}(\mathbf{3})](\text{OTf})_2$  with  $\text{H}_2\text{O}_2$  in MeCN.

$k \cdot [\text{H}_2\text{O}_2]$ ). Therefore, it leads to an overall second order rate law and from the slopes the second order rate constants were obtained that could be used for an Eyring plot (see Supporting Information, Figure S2). From the Eyring plot activation parameters were calculated leading to  $\Delta H^\ddagger = 28 \pm 4\text{ kJ}\cdot\text{mol}^{-1}$  and an activation entropy of  $\Delta S^\ddagger = -144 \pm 15\text{ J}\cdot\text{mol}^{-1}\cdot\text{K}^{-1}$ . The strongly negative activation entropy supports an associative mechanism. From the kinetic data we can postulate an overall mechanism that is shown in Scheme 3. The kinetic data clearly show that in a first associative step



**Scheme 3.** Proposed mechanism for the formation of  $[\text{Fe}(\text{3})(\text{O})](\text{OTf})_2$ .

hydrogen peroxide coordinates to the iron complex. Only *cis*-binding (observed for O-atom exchange described previously) [27] of the hydrogen peroxide is possible due to the fact that the *trans* position is already blocked by the amide group of the ligand. The reaction is the rate determining step and therefore the consecutive reactions are fast and cannot be observed in detail in our kinetic study. However, Hirao *et al.* described in a theoretical study the O-O cleavage leading to the oxido iron(IV) complex through a hydrogen atom transfer reaction (Scheme 3, with no additional base present) [28].

#### 2.4. Fe(II) complexes with DMEG<sub>3</sub>tren (**4**) as a ligand

As described in the introduction, the tripodal ligand TMG<sub>3</sub>tren was used to structurally characterize a high-spin oxido iron(IV) complex. Its fully deuterated form, d<sub>36</sub>-TMG<sub>3</sub>tren, had to be used to avoid hydroxylation of one of the methyl groups at the guanidine nitrogen [15]. Trying to improve the stability of the oxido iron(IV) complex further, we applied DMEG<sub>3</sub>tren (**4**, Scheme 1) that is a sterically more restrictive derivative of TMG<sub>3</sub>tren [16]. The reported synthesis of **4** could be modified to obtain the ligand in a facile way in good yields without the necessity to apply phosgene [29].

The iron(II) complex  $[\text{Fe}(\mathbf{4})(\text{MeCN})](\text{OTf})_2$  was obtained by reacting  $\text{Fe}(\text{MeCN})_2(\text{OTf})_2$  with DMEG<sub>3</sub>tren in acetonitrile. The molecular structure of this complex is presented in Figure 5 (left). Removal of the coordinated acetonitrile was achieved by recrystallization from dcm as described previously [8]. The molecular structure of  $[\text{Fe}(\mathbf{4})(\text{OTf})](\text{OTf})$  is presented in Figure 5 (right). Crystallographic data of both complexes are reported in the Supporting Information. The molecular structure of  $[\text{Fe}(\mathbf{4})(\text{OTf})](\text{OTf})$  is very similar to the molecular structure of  $[\text{Fe}(\text{TMG}_3\text{tren})(\text{OTf})](\text{OTf})$  reported previously. However, while reactions of both complexes with either ozone or hydrogen peroxide were observed, we did not succeed in obtaining the oxido iron complex,  $[\text{Fe}(\mathbf{4})(\text{O})](\text{OTf})_2$ , as a product yet.

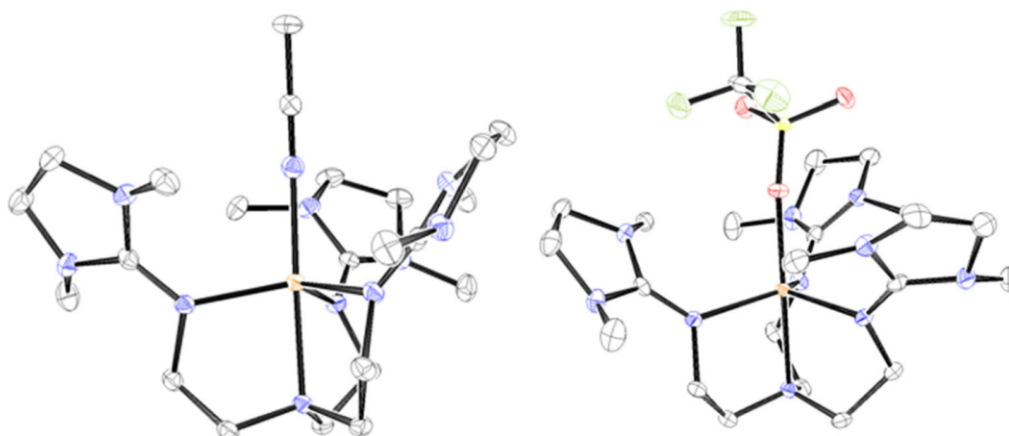


**Figure 5.** ORTEP plots of the cations of the molecular structures of  $[\text{Fe}(\mathbf{4})(\text{MeCN})](\text{OTf})_2$  (left) and  $[\text{Fe}(\mathbf{4})(\text{OTf})](\text{OTf})$  (right); anions and solvent molecules are omitted for clarity.

### 2.5. Cr(II) Complexes with DMEG<sub>3</sub>tren (**4**) as a ligand

Chromium complexes can be used to model the reactivity of iron enzymes. For example Nam and co-workers reported a chromium(III) superoxido complex that was applied as a biomimetic model compound for the proposed iron superoxido species in the active site of cysteine dioxygenase [30]. Furthermore, TMG<sub>3</sub>tren is quite useful to stabilize otherwise reactive "dioxygen adduct" complexes. Thus we had applied TMG<sub>3</sub>tren to obtain the first *end-on*-superoxido copper complex that could be structurally characterized [13]. Superoxides are related to ozonides and alkali ozonides can be synthetically prepared from alkali superoxides by reacting them with ozone [23, 24]. With this background we thought it could be possible to obtain an ozonido chromium(III) complex from the reaction of ozone with a corresponding chromium(II) complex. Chromium(III) complexes are kinetically inert and therefore it seemed likely that such an intermediate could be stable enough to isolate it prior to its further reaction to an oxido complex.

The synthesis of the chromium precursor complexes with DMEG<sub>3</sub>tren as a ligand was performed similar to the Fe(II) analogues in MeCN. A complex with a coordinating acetonitrile and two triflate anions was obtained and structurally characterized (Figure 6, left). An attempt to remove the solvent molecule by recrystallization from dcm led to a Cl<sup>-</sup> abstraction reaction and the Cr(II) complex with a coordinated chloride anion was obtained (Figure 6, right). Crystallographic data for both complexes are reported in the Supporting Information. Unfortunately, so far all our efforts to crystallize either a superoxido (from the reaction with dioxygen), an ozonido or an oxido complex from the reactions of  $[\text{Cr}(\mathbf{4})(\text{MeCN})](\text{OTf})_2$  have failed.

### 3. Conclusion

For the synthesis of oxido iron(IV) complexes different oxidants can be used such as, for example, hydrogen peroxide or iodoso benzene. Hydrogen peroxide has the disadvantage to introduce water into the reaction and iodoso benzene is known for difficulties in solubility (this has been somewhat improved by applying derivatives). We recently started to apply ozone as a "clean" oxidant that offers several advantages in synthetic applications.

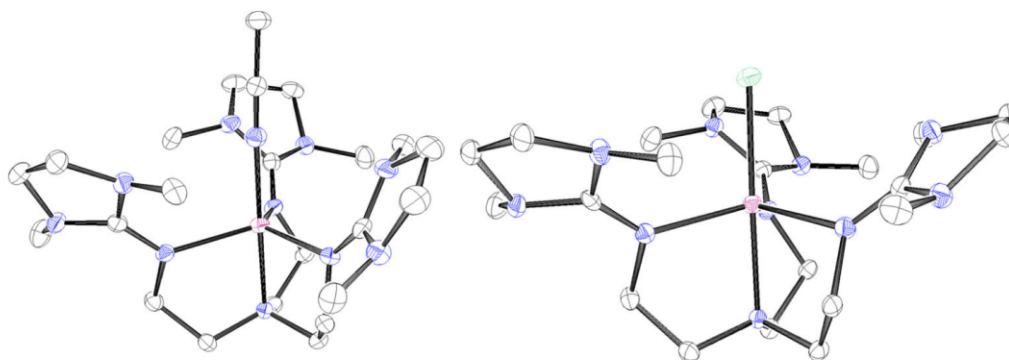


**Figure 6.** ORTEP plots of the cations of the  $\text{Cr}^{2+}$  complexes with ligand **4**, with an additional MeCN ligand (left) and a  $\text{Cl}^-$  ligand (right). Hydrogen atoms and anion molecules are omitted for clarity.

Unfortunately, due to the fact that ozone only can be supplied in a mixture with dioxygen in a quite low concentration, kinetic studies are limited or not possible. In addition, if the complexes already react with dioxygen alone things are even more complicated. A general limitation – for all oxidants – are the solvents: acetonitrile is a quite strongly coordinating solvent that can suppress reactions and furthermore only allows low temperatures close to  $-40^\circ\text{C}$  (furthermore cyanide can form); dcm, stable towards ozone, is a non-coordinating solvent, allowing measurements at lower temperatures, however, chloride abstraction can easily occur (as observed for the chromium complex described above). Other solvents such as, for example, THF often show decomposition reactions with the oxidants.

However, while we could not study the kinetics of reactions with ozone it was possible to obtain kinetic data by stopped-flow measurements for the reaction of  $[\text{trans-}[\text{Fe}(\text{Cyclam})(\text{MeCN})_2](\text{OTf})_2]$  with dioxygen and the iron(II) complex with an amide derivative of tetramethylcyclam (TMC) as ligand together with hydrogen peroxide. Especially interesting is the two step mechanism for the reaction  $[\text{trans-}[\text{Fe}(\text{Cyclam})(\text{MeCN})_2](\text{OTf})_2]$  with dioxygen, forming in a first step a superoxido iron(III) complex prior to the formation of the oxido iron(IV) complex in the second step. No further intermediates, such as a postulated peroxido complex, could be spectroscopically observed. A large negative activation entropy of  $\Delta S^\ddagger = -144 \pm 15 \text{ J} \cdot \text{mol}^{-1} \cdot \text{K}^{-1}$  for the reaction of the iron(II) amide TMC complex with hydrogen peroxide supports an associative mechanism. Thus it is clear that the rate determining step is the associative binding of hydrogen peroxide followed by fast consecutive steps to formation of the oxido Fe(IV) complex. The postulated mechanisms should be quite helpful for a better understanding of the general mechanisms for oxidation of iron(II) complexes and provide information for future applications in catalytic oxidation reactions.

Unfortunately, our expectations to obtain a more stable oxido iron(IV) complex with the tripodal ligand DMEG<sub>3</sub>tren or to isolate an ozonido iron or chromium complex as an intermediate were not successful. Most likely oxidation of the ligand is a problem.

## 4. Experimental

### 4.1. General methods

Commercially available reagents were used as obtained without purification, unless otherwise stated. Anhydrous solvents were purchased from Acros Organics and further

distilled three times over drying agents under Schlenk conditions. All experiments with air-sensitive compounds were carried out employing standard Schlenk techniques or by working in a glove box (MBraun, Garching, Germany; O<sub>2</sub> and H<sub>2</sub>O < 0.1 ppm) under an argon atmosphere. Ligand **3** was prepared as described previously [11]. The complexes [Fe(**2**)(OTf)](OTf) [8], *trans*-[Fe(**1**)(MeCN)<sub>2</sub>](OTf)<sub>2</sub> [10] and [Fe(**3**)](OTf)<sub>2</sub> [11] were synthesized according to the corresponding published procedures.

#### 4.2. Low-temperature stopped-flow measurements

Variable temperature stopped-flow measurements allowed the collection of time-resolved UV-vis spectra of the reactions of the precursor complex with the corresponding oxidants as described previously [31]. The solutions were prepared in a glove box and transferred to the low-temperature stopped-flow instrument using gas tight glass syringes. All reactions were typically studied under pseudo-first-order conditions with an excess of the oxidant. Temperatures varied in a range from -80 to -10 °C depending on the solvent used. Time-resolved UV-vis spectra of these reactions were recorded with a Hi-Tech SF-61SX2 low-temperature stopped-flow unit equipped with a diode array spectrophotometer (Hi-Tech, Salisbury, UK; now TgK Scientific, Bradford-on-Avon, UK). Details on the setup and kinetic measurements have been described previously [32]. Data fitting was performed using the integrated Kinetic Studio 4.0 software package (TgK Scientific, Bradford-on-Avon, UK) and Origin 2018 (OriginLab Corporation, Northampton, USA).

#### 4.3. Single-crystal X-ray structure determinations

Diffraction data for all samples were collected at low temperatures (100 K) using  $\varphi$ - and  $\omega$ -scans on a BRUKER D8 Venture System equipped with dual  $\lambda$  microfocus sources, a PHOTON100 detector and an OXFORD CRYOSYSTEMS 700 low temperature system. Mo-K $\alpha$  radiation with a wavelength of 0.71073 Å and a collimating Quazar multilayer mirror were used. Details of the crystal structure refinement and structural parameters are described in the Supporting Information.

The crystallographic data have been deposited with the Cambridge Crystallographic Data Centre as CCDC Nos. 2128924-2128929 and can be obtained free of charge (<https://www.ccdc.cam.ac.uk/structures/>).

#### 4.4. Synthesis of DMEG<sub>3</sub>tren (**4**)

The synthesis was modified based on a reported procedure [29]. In 35 mL abs. MeCN 877 mg of tris(2-aminoethyl)amine (tren) (6.00 mmol) and 1.821 g Et<sub>3</sub>N (18.00 mmol) were dissolved and the solution was cooled to 0 °C under Schlenk conditions. Under vigorous stirring a solution of 3.043 g 2-chloro-1,3-dimethylimidazolium chloride (DMC) (20.30 mmol) in 15 mL of dcm was added via a syringe over 30 min and a colorless precipitate formed. After completion, the mixture was stirred for an additional 30 min at 0 °C and after warmup refluxed for another 18 h. At rt 18 mL of 1 M NaOH solution (18 mmol) was added to the reaction suspension and the solid dissolved. The

obtained two-phase solution was reduced to dryness to remove solvents, water and trimethylamine. The obtained residue was treated with 30 mL 50% KOH solution and extracted with 30 mL of MeCN three times. The united organic phases were dried over NaSO<sub>4</sub> and the solvents were removed in vacuo. Under inert conditions the yellow oil obtained was dissolved in 5 mL of abs. Et<sub>2</sub>O and dried over 4 Å molecular sieves overnight. The solution was filtered and reduced to dryness. The crude product was again dissolved in abs. dcm, treated with a twofold amount of abs. Et<sub>2</sub>O and crystallized at -30 °C for 18 h. The solution was decanted, the obtained crystals washed with abs. Et<sub>2</sub>O and dried in vacuo. 1.598 g (3.677 mmol) of the solid ligand in form of white crystals were obtained (61%). <sup>1</sup>H NMR (400 MHz, CDCl<sub>3</sub>): δ = 3.52–3.48 (m, 6 H, CH<sub>2</sub>), 3.10 (s, 12 H, N-CH<sub>2</sub>-CH<sub>2</sub>-N), 2.85–2.65 (m, 24 H, CH<sub>2</sub>, CH<sub>3</sub>). <sup>13</sup>C (100 MHz, CDCl<sub>3</sub>): δ = 157.5, 59.0, 50.8, 48.2, 46.4, 38.3, 34.6.

#### 4.5. Synthesis of [Fe(4)(MeCN)](OTf)<sub>2</sub>

In 10 mL of MeCN 251 mg Fe(MeCN)<sub>2</sub>(OTf)<sub>2</sub> (0.575 mmol) and 250 mg DMEG<sub>3</sub>tren (0.575 mmol) were dissolved and stirred overnight. The colorless solution was reduced to ca. 2 mL in vacuo, an excess of Et<sub>2</sub>O was added and then stored at -40 °C for crystallization. After five days suitable crystals could be obtained as colorless blocks, which were filtered and dried (404 mg, 85%).

#### 4.6. Synthesis of [Fe(4)(OTf)](OTf)

The coordinated MeCN molecule in [Fe(4)(MeCN)](OTf)<sub>2</sub> was removed by recrystallization from dcm. In 5 mL of dcm 404 mg [Fe(DMEG<sub>3</sub>tren)(MeCN)](OTf)<sub>2</sub> (0.487 mmol) was dissolved and heated. To the colorless solution 5 mL of *n*-pentane was added and it was stored at -40 °C for crystallization. After three days, 295 mg of colorless crystals were isolated and dried in vacuo (0.374 mmol, 77%). Elemental analysis of 4-Fe calculated for C<sub>23</sub>H<sub>42</sub>F<sub>6</sub>FeN<sub>10</sub>O<sub>6</sub>S<sub>2</sub> (788.608 g/mol): C 35.03%, H 5.37%, N 17.76%; found: C 35.00%, H 5.35%, N 17.42%.

#### 4.7. Synthesis of Cr(MeCN)<sub>2</sub>(OTf)<sub>2</sub>

The synthesis was optimized based on a literature procedure [33]. In 70 mL of abs. MeCN 10.00 g CrCl<sub>2</sub> (81.36 mmol) was suspended. Under stirring, 70.00 mL trimethylsilyl trifluoromethanesulfonate (86.00 g, 386.9 mmol) was added. The solution turned slowly blue and was stirred at rt for 18 h. The volatiles were removed in vacuo and the light-blue residue was taken up in 30 mL abs. MeCN and filtered. The intensive blue filtrate was layered with Et<sub>2</sub>O and stored at -40 °C for crystallization for several days. The dark blue crystals were isolated and dried in vacuo and 22.15 g product was obtained as a light blue powder (63%).

#### 4.8. Synthesis of [Cr(4)(MeCN)](OTf)<sub>2</sub>

To a solution of 870 mg DMEG<sub>3</sub>tren (2.00 mmol) in 10 mL of MeCN, a solution of 886 mg Cr(MeCN)<sub>2</sub>(OTf)<sub>2</sub> (2.05 mmol) in 5 mL of MeCN was added dropwise. The deep blue solution was stirred for an additional 30 min at rt, then layered with Et<sub>2</sub>O and stored at –30 °C for several days. The obtained blue crystals 1.366 g were filtered and the solid dried in vacuo (83%). Elemental analysis of **4**-Cr calculated for C<sub>23</sub>H<sub>42</sub>CrF<sub>6</sub>N<sub>10</sub>O<sub>6</sub>S<sub>2</sub> (784.760 g/mol): C 35.20%, H 5.39%, N 17.85%; found: C 35.75%, H 5.60%, N 17.87%.

#### Acknowledgements

We gratefully acknowledge support by the Justus-Liebig-Universität Gießen and the Deutsche Forschungsgemeinschaft for financial support (SS, SCHI 377/18-1). Furthermore, we would like to thank Stefan Schaub for his expertise in the practical handling of ozone in the laboratory.

#### Disclosure statement

No potential conflict of interest was reported by the authors.

#### ORCID

Siegfried Schindler  <http://orcid.org/0000-0002-9991-9513>

#### References

- [1] M. Guo, T. Corona, K. Ray, W. Nam. *ACS Cent. Sci.*, **5**, 13 (2019).
- [2] X. Lu, X.-X. Li, Y.-M. Lee, Y. Jang, M.S. Seo, S. Hong, K.-B. Cho, S. Fukuzumi, W. Nam. *J. Am. Chem. Soc.*, **142**, 3891 (2020).
- [3] W. Nam. *Acc. Chem. Res.*, **48**, 2415 (2015).
- [4] X. Engelmann, I. Monte-Pérez, K. Ray. *Angew. Chem. Int. Ed.*, **55**, 7632 (2016).
- [5] J.-U. Rohde, J.-H. In, M.H. Lim, W.W. Brennessel, M.R. Bukowski, A. Stubna, E. Münck, W. Nam, L. Que. *Science*, **299**, 1037 (2003).
- [6] H. Park, D. Lee. *Chem. Eur. J.*, **26**, 5916 (2020).
- [7] X. Engelmann, D.D. Malik, T. Corona, K. Warm, E.R. Farquhar, M. Swart, W. Nam, K. Ray. *Angew. Chem. Int. Ed.*, **58**, 4012 (2019).
- [8] S. Schaub, A. Miska, J. Becker, S. Zahn, D. Mollenhauer, S. Sakshath, V. Schünemann, S. Schindler. *Angew. Chem. Int. Ed.*, **57**, 5355 (2018).
- [9] O. Pestovsky, S. Stoian, E.L. Bominaar, X. Shan, E. Münck, L. Que, A. Bakac. *Angew. Chem. Int. Ed.*, **42**, 6871 (2005); C.A. Grapperhaus, B. Mienert, E. Bill, T. Weyhermüller, K. Wieghardt. *Inorg. Chem.*, **23**, 5306 (2000).
- [10] D. Kass, T. Corona, K. Warm, B. Braun-Cula, U. Kuhlmann, E. Bill, S. Mebs, M. Swart, H. Dau, M. Haumann, P. Hildebrandt, K. Ray. *J. Am. Chem. Soc.*, **142**, 5924 (2020).
- [11] J. England, J.O. Bigelow, K.M. van Heuvelen, E.R. Farquhar, M. Martinho, K.K. Meier, J.R. Frisch, E. Münck, L. Que. *Chem. Sci.*, **5**, 1204 (2014).
- [12] H. Wittmann, V. Raab, A. Schorm, J. Plackmeyer, J. Sundermeyer. *Eur. J. Inorg. Chem.*, **8**, 1937 (2001); R.L. Peterson, J.W. Ginsbach, R.E. Cowley, M.F. Qayyum, R.A. Himes, M.A. Siegler, C.D. Moore, B. Hedman, K.O. Hodgson, S. Fukuzumi, E.I. Solomon, K.D. Karlin. *J. Am. Chem. Soc.*, **44**, 16454 (2013).

- [13] C. Würtele, E. Gaoutchenova, K. Harms, M.C. Holthausen, J. Sundermeyer, S. Schindler. *Angew. Chem. Int. Ed.*, **45**, 3867 (2006).
- [14] J. England, M. Martinho, E.R. Farquhar, J.R. Frisch, E.L. Bominaar, E. Münck, L. Que. *Angew. Chem. Int. Ed.*, **48**, 3622 (2009).
- [15] J. England, Y. Guo, E.R. Farquhar, V.G. Young, E. Münck, L. Que. *J. Am. Chem. Soc.*, **132**, 8635 (2010).
- [16] G.F. Payne, P.B. Smith (Eds.), *Renewable and Sustainable Polymers*, Oxford University Press Inc, New York (2011).
- [17] S. Hong, Y.-M. Lee, K. Ray, W. Nam. *Coord. Chem. Rev.*, **334**, 25 (2017).
- [18] T. Hoppe, S. Schaub, J. Becker, C. Würtele, S. Schindler. *Angew. Chem. Int. Ed.*, **52**, 870 (2013); J. Müller, C. Würtele, O. Walter, S. Schindler. *Angew. Chem. Int. Ed.*, **41**, 7775 (2007).
- [19] J.H. Espenson (Ed.), *Chemical Kinetics and Reaction Mechanisms*, McGraw-Hill, New York (1995).
- [20] M. Lerch, M. Weitzer, T.-D.J. Stumpf, L. Laurini, A. Hoffmann, J. Becker, A. Miska, R. Göttlich, S. Herres-Pawlis, S. Schindler. *Eur. J. Inorg. Chem.*, **2020**, 3143 (2020).
- [21] A. Hazell, C.J. McKenzie, L.P. Nielsen, S. Schindler, M. Weitzer. *J. Chem. Soc., Dalton Trans.*, 310 (2002); J. Kaizer, E.J. Klinker, N.Y. Oh, J.-U. Rohde, W.J. Song, A. Stubna, J. Kim, E. Münck, W. Nam, L. Que. *J. Am. Chem. Soc.*, **2**, 472 (2004).
- [22] J. Cho, R. Sarangi, W. Nam. *Acc. Chem. Res.*, **45**, 1321 (2012).
- [23] M. Jansen, H. Nuss. *Z. anorg. allg. Chem.*, **633**, 1307 (2007).
- [24] W. Schnick, M. Jansen. *Angew. Chem. Int. Ed.*, **24**, 54 (1985).
- [25] G. Royal, V. Dahaoui-Gindrey, S. Dahaoui, A. Tabard, R. Guilard, P. Pullumbi, C. Lecomte. *Eur. J. Org. Chem.*, **1998**, 1971 (1998).
- [26] C. Bucher, E. Duval, J.-M. Barbe, J.-N. Verpeaux, C. Amatore, R. Guilard. *C. R. Acad. Sci. Paris, Chim./Chem.*, **3**, 211 (2000).
- [27] M.S. Seo, J.-H. In, S.O. Kim, N.Y. Oh, J. Hong, J. Kim, L. Que, W. Nam. *Angew. Chem. Int. Ed.*, **43**, 2417 (2004).
- [28] H. Hirao, F. Li, L. Que, K. Morokuma. *Inorg. Chem.*, **50**, 6637 (2011).
- [29] E.V. Gauchenova. *Chemie superbasischer Chelatliganden für H<sup>+</sup>, Cu<sup>+</sup> und Mn<sup>2+</sup>*, Dissertation (2006).
- [30] J. Cho, J. Woo, W. Nam. *J. Am. Chem. Soc.*, **134**, 11112 (2012).
- [31] M. Lerch, A.J. Achazi, D. Mollenhauer, J. Becker, S. Schindler. *Eur. J. Inorg. Chem.*, **2021**, 4122 (2021).
- [32] M. Weitzer, M. Schatz, F. Hampel, F.W. Heinemann, S. Schindler. *J. Chem. Soc., Dalton Trans.*, 686 (2002).
- [33] A. Zhou, S.T. Kleespies, K.M. van Heuvelen, L. Que. *Chem. Commun.*, **51**, 14326 (2015).

## 5. References

- [1] J. N. Armor, *Catal. Today* **2011**, 163, 3.
- [2] Climate Change Technology Program, *Industrial Process Efficiency. Commercialization and Deployment Activities*, **2005**, 1.4-7 - 1.4.9.
- [3] J. Wisniak, *Educ. Quim.* **2010**, 21, 60.
- [4] Dr. Moncef Hadhri, "The European Chemical industry Facts and Figures 2023", can be found under <https://cefic.org/app/uploads/2023/03/2023-Facts-and-Figures.pdf>, **2023**.
- [5] a) G. J. Leigh in *Catalysts for Nitrogen Fixation* (Eds.: B. E. Smith, R. L. Richards, W. E. Newton), Springer Netherlands, Dordrecht, **2004**, pp. 33–54; b) F. Haber, G. van Oordt, *Z. Anorg. Chem.* **1905**, 44, 341.
- [6] a) R. Schlögl, *Angew. Chem. Int. Ed.* **2003**, 115, 2050; b) T. Rayment, R. Schlögl, J. M. Thomas, G. Ertl, *Nature* **1985**, 315, 311.
- [7] Dietrich Stoltzenberg, *Chem. unserer Zeit* **1999**, 33, 359.
- [8] M. Appl in *Ullmann's Encyclopedia of Industrial Chemistry*, Wiley-VCH Verlag GmbH & Co. KGaA, Weinheim, Germany, **2000**.
- [9] M. Appl in *Ullmann's Encyclopedia of Industrial Chemistry*, Wiley-VCH Verlag GmbH & Co. KGaA, Weinheim, Germany, **2000**.
- [10] BASF SE, "Ammoniakanlage am Standort Ludwigshafen", can be found under [https://www.basf.com/global/de/media/events/2019/full-year-results/photos-pk.fragment.html/overview\\_copy\\_copy\\_c\\$/global/press-photos/de/photos/2019/02/annual-press-conference/10\\_5114\\_Ammonia\\_plant\\_at\\_Ludwigshafen\\_site.jpg.html](https://www.basf.com/global/de/media/events/2019/full-year-results/photos-pk.fragment.html/overview_copy_copy_c$/global/press-photos/de/photos/2019/02/annual-press-conference/10_5114_Ammonia_plant_at_Ludwigshafen_site.jpg.html).
- [11] J. Humphreys, R. Lan, S. Tao, *Adv. Energy Sustain. Res.* **2021**, 2, 2000043.
- [12] G. Soloveichik, *Nat. Catal.* **2019**, 2, 377.
- [13] N. Cherkasov, A. O. Ibadon, P. Fitzpatrick, *Chem. Eng. Process.* **2015**, 90, 24.
- [14] H. Hirakawa, M. Hashimoto, Y. Shiraishi, T. Hirai, *J. Am. Chem. Soc.* **2017**, 139, 10929.
- [15] J. A. Kurzman, L. M. Misch, R. Seshadri, *Dalton Trans.* **2013**, 42, 14653.
- [16] W. Keim, *Angew. Chem. Int. Ed.* **1990**, 29, 235.
- [17] *Organometallics in synthesis. Fourth manual*, John Wiley & Sons, Hoboken, New Jersey, **2013**.

- [18] A. E. King, S. C. E. Stieber, N. J. Henson, S. A. Kozimor, B. L. Scott, N. C. Smythe, A. D. Sutton, J. C. Gordon, *Eur. J. Inorg. Chem.* **2016**, 2016, 1635.
- [19] G. Wilke, *Angew. Chem. Int. Ed.* **1988**, 27, 185.
- [20] K. Fischer, K. Jonas, P. Misbach, R. Stabba, G. Wilke, *Angew. Chem. Int. Ed.* **1973**, 12, 943.
- [21] S. Z. Tasker, E. A. Standley, T. F. Jamison, *Nature* **2014**, 509, 299.
- [22] P. R. Chopade, J. Louie, *Adv. Synth. Catal.* **2006**, 348, 2307.
- [23] J. Montgomery, *Angew. Chem. Int. Ed.* **2004**, 43, 3890.
- [24] T. van Tran, Z.-Q. Li, O. Apolinar, J. Derosa, M. V. Joannou, S. R. Wisniewski, M. D. Eastgate, K. M. Engle, *Angew. Chem. Int. Ed.* **2020**, 59, 7409.
- [25] L. Nattmann, R. Saeb, N. Nöthling, J. Cornella, *Nat. Catal.* **2020**, 3, 6.
- [26] A. J. Nett, S. Cañellas, Y. Higuchi, M. T. Robo, J. M. Kochkodan, M. T. Haynes, J. W. Kampf, J. Montgomery, *ACS Catal.* **2018**, 8, 6606.
- [27] E. A. Standley, S. J. Smith, P. Müller, T. F. Jamison, *Organometallics* **2014**, 33, 2012.
- [28] F. Alonso, P. Riente, M. Yus, *Acc. Chem. Res.* **2011**, 44, 379.
- [29] W. Kaim, *Bioanorganische Chemie. Zur Funktion chemischer Elemente in Lebensprozessen*, Vieweg+Teubner Verlag, Wiesbaden, **2005**.
- [30] L. M. Mirica, X. Ottenwaelder, T. D. P. Stack, *Chem. Rev.* **2004**, 104, 1013.
- [31] W. Kaim, J. Rall, *Angew. Chem. Int. Ed.* **1996**, 35, 43.
- [32] U. Ermler, W. Grabarse, S. Shima, M. Goubeaud, R. K. Thauer, *Curr. Opin. Struct. Biol.* **1998**, 8, 749.
- [33] N. E. Dixon, T. C. Gazzola, R. L. Blakeley, B. Zermer, *J. Am. Chem. Soc.* **1975**, 97, 4131.
- [34] M. J. Maroney, S. Ciurli, *Chem. Rev.* **2014**, 114, 4206.
- [35] S. W. Ragsdale, *Curr. Opin. Chem. Biol.* **1998**, 2, 208.
- [36] S. W. Ragsdale, *J. Biol. Chem.* **2009**, 284, 18571.
- [37] H. D. Youn, E. J. Kim, J. H. Roe, Y. C. Hah, S. O. Kang, *Biochem. J.* **1996**, 318 ( Pt 3), 889.
- [38] M. E. Krause, A. M. Glass, T. A. Jackson, J. S. Laurence, *Inorg. Chem.* **2010**, 49, 362.

- [39] J. L. Boer, S. B. Mulrooney, R. P. Hausinger, *Arch. Biochem. Biophys.* **2014**, *544*, 142.
- [40] a) A. T. Fiedler, P. A. Bryngelson, M. J. Maroney, T. C. Brunold, *J. Am. Chem. Soc.* **2005**, *127*, 5449; b) J. Wuerges, J.-W. Lee, Y.-I. Yim, H.-S. Yim, S.-O. Kang, K. Djinnovic Carugo, *Proc. Natl. Acad. Sci. U S A* **2004**, *101*, 8569.
- [41] W. Ternes, *Biochemie der Elemente*, Springer Berlin Heidelberg, Berlin, Heidelberg, **2013**.
- [42] A. L. Feig, S. J. Lippard, *Chem. Rev.* **1994**, *94*, 759.
- [43] R. H. Holm, P. Kennepohl, E. I. Solomon, *Chem. Rev.* **1996**, *96*, 2239.
- [44] Richard Wheeler (Zephyris), "Hemoglobin. (heterotetramer, ( $\alpha\beta$ )<sub>2</sub>)", can be found under [https://en.wikipedia.org/wiki/Hemoglobin#/media/File:1GZX\\_Haemoglobin.png](https://en.wikipedia.org/wiki/Hemoglobin#/media/File:1GZX_Haemoglobin.png), **2007**.
- [45] J. Hohenberger, K. Ray, K. Meyer, *Nat. Commun.* **2012**, *3*, 720.
- [46] J. L. Que, M. Puri, *Bull. Jpn. Soc. Coord. Chem.* **2016**, *67*, 10.
- [47] M. Guo, T. Corona, K. Ray, W. Nam, *ACS Cent. Sci.* **2019**, *5*, 13.
- [48] a) J. M. Bollinger, J. C. Price, L. M. Hoffart, E. W. Barr, C. Krebs, *Eur. J. Inorg. Chem.* **2005**, *2005*, 4245; b) E. I. Solomon, T. C. Brunold, M. I. Davis, J. N. Kemsley, S. K. Lee, N. Lehnert, F. Neese, A. J. Skulan, Y. S. Yang, J. Zhou, *Chem. Rev.* **2000**, *100*, 235; c) T. L. Poulos, *Chem. Rev.* **2014**, *114*, 3919; d) E. I. Solomon, A. Decker, N. Lehnert, *Proc. Natl. Acad. Sci. U S A* **2003**, *100*, 3589; e) E. I. Solomon, S. Goudarzi, K. D. Sutherland, *Biochemistry* **2016**, *55*, 6363; f) S. J. Lange, L. Que, *Curr. Opin. Chem. Biol.* **1998**, 159.
- [49] L. Que, *J Biol. Inorg. Chem.* **2017**, *22*, 171.
- [50] A. S. Borovik, P. J. Zinn, M. K. Zart, *Dioxygen Binding and Activation: Reactive Intermediates*, **2006**.
- [51] X. Liu, Y. Ryabenkova, M. Conte, *Phys. Chem. Chem. Phys.* **2015**, *17*, 715.
- [52] W. T. Borden, R. Hoffmann, T. Stuyver, B. Chen, *Journal of the American Chemical Society* **2017**, *139*, 9010.
- [53] W. Nam, *Acc. Chem. Res.* **2007**, *40*, 522.
- [54] Y. Gong, M. Zhou, L. Andrews, *Chem. Rev.* **2009**, *109*, 6765.
- [55] K. Ray, F. F. Pfaff, B. Wang, W. Nam, *J. Am. Chem. Soc.* **2014**, *136*, 13942.
- [56] S. Itoh, *Acc. Chem. Res.* **2015**, *48*, 2066.

- [57] B. Kim, K. D. Karlin, *Acc. Chem. Res.* **2023**, *56*, 2197.
- [58] C. E. MacBeth, A. P. Golombek, V. G. Young, C. Yang, K. Kuczera, M. P. Hendrich, A. S. Borovik, *Science* **2000**, *289*, 938.
- [59] J.-U. Rohde, J.-H. In, M. H. Lim, W. W. Brennessel, M. R. Bukowski, A. Stubna, E. Münck, W. Nam, L. Que, *Science* **2003**, *299*, 1037.
- [60] J. Cho, S. Jeon, S. A. Wilson, L. V. Liu, E. A. Kang, J. J. Braymer, M. H. Lim, B. Hedman, K. O. Hodgson, J. S. Valentine et al., *Nature* **2011**, *478*, 502.
- [61] A. Thibon, J. England, M. Martinho, V. G. Young, J. R. Frisch, R. Guillot, J.-J. Girerd, E. Münck, L. Que, F. Banse, *Angew. Chem. Int. Ed.* **2008**, *47*, 7064.
- [62] J. England, J. O. Bigelow, K. M. van Heuvelen, E. R. Farquhar, M. Martinho, K. K. Meier, J. R. Frisch, E. Münck, L. Que, *Chem. Sci.* **2014**, *5*, 1204.
- [63] S. Schaub, A. Miska, J. Becker, S. Zahn, D. Mollenhauer, S. Sakshath, V. Schünemann, S. Schindler, *Angew. Chem. Int. Ed.* **2018**, *57*, 5355.
- [64] S. M. Barry, G. L. Challis, *ACS Catal.* **2013**, *3*.
- [65] D. Kass, T. Corona, K. Warm, B. Braun-Cula, U. Kuhlmann, E. Bill, S. Mebs, M. Swart, H. Dau, M. Haumann et al., *J. Am. Chem. Soc.* **2020**, *142*, 5924.
- [66] D. K. Cabbiness, D. W. Margerum, *J. Am. Chem. Soc.* **1969**, *91*, 6540.
- [67] T. Rotärmel, J. Becker, S. Schindler, *Faraday Discuss.* **2022**, *234*, 70.
- [68] J. van Alphen, *Recl. Trav. Chim. Pays-Bas* **1937**, *56*, 343.
- [69] H. Stetter, K.-H. Mayer, *Chem. Ber.* **1961**, *94*, 1410.
- [70] a) A. K. Holanda, F. O. Da Silva, I. M. Carvalho, A. A. Batista, J. Ellena, E. E. Castellano, Í. S. Moreira, L. G. Lopes, *Polyhedron* **2007**, *26*, 4653; b) S. S. Isied, *Inorg. Chem.* **1980**, *19*, 911; c) B. Bosnich, M. L. Tobe, G. A. Webb, *Inorg. Chem.* **1965**, *4*, 1109; d) P. A. Daugherty, J. Glerup, P. A. Goodson, D. J. Hodgson, K. Michelsen, E. Kleinpeter, *Acta Chem. Scand.* **1991**, *45*, 244; e) P. A. Tasker, L. Sklar, *J. Mol. Struct.* **1975**, *5*, 329; f) B. Bosnich, C. K. Poon, M. L. Tobe, *Inorg. Chem.* **1965**, *4*, 1102.
- [71] E. K. Barefield, F. Wagner, *Inorg. Chem.* **1973**, *12*, 2435.
- [72] a) A. T. Fiedler, H. L. Halfen, J. A. Halfen, T. C. Brunold, *J. Am. Chem. Soc.* **2005**, *127*, 1675; b) M. R. Bukowski, K. D. Koehntop, A. Stubna, E. L. Bominaar, J. A. Halfen, E. Münck, W. Nam, L. Que, *Science* **2005**, *310*, 1000.

- [73] L. Siegfried, C. N. McMahon, J. Baumeister, M. Neuburger, T. A. Kaden, S. Anandaram, C. G. Palivan, *Dalton Trans.* **2007**, 4797.
- [74] a) L. Siegfried, C. N. McMahon, T. A. Kaden, C. Palivan, G. Gescheidt, *Dalton Trans.* **2004**, 2115; b) L. Siegfried, M. Honecker, A. Schlageter, T. A. Kaden, *Dalton Trans.* **2003**, 3939.
- [75] a) C. Geyer, E. Dinjus, S. Schindler, *Organometallics* **1998**, *17*, 98; b) C. Geyer, S. Schindler, *Organometallics* **1998**, *17*, 4400; c) Helmut Weiss, *Dissertation*, Friedrich-Alexander-Universität Erlangen-Nürnberg, Erlangen, **2001**.
- [76] H. Weiss, F. Hampel, W. Donaubaue, M. A. Grundl, J. W. Bats, A. S. K. Hashmi, S. Schindler, *Organometallics* **2001**, *20*, 1713.

## 5.1 Copyright References

**Figure 3:** [39] Reprinted from Archives of Biochemistry and Biophysics, Nickel-dependent metalloenzymes, J. L. Boer, S. B. Mulrooney, R. P. Hausinger, **2014**, *544*, 146, with permission from Elsevier.

**Chapter 4:** © copyright # **2023**, reprinted by permission of Informa UK Limited, trading as Taylor & Taylor & Francis Group, <http://www.tandfonline.com>